



MASTERARBEIT / MASTER'S THESIS

Titel der Masterarbeit / Title of the Master's Thesis

“Developmental neurotoxicity of perinatal exposure
to HexaBromoCycloDoDecane with regard to its impact
on epigenetics and neuroinflammation “

verfasst von / submitted by

Sarah Roth, BSc

angestrebter akademischer Grad / in partial fulfilment of the requirements for the degree of
Master of Science (MSc)

Wien, 2019 / Vienna, 2019

Studienkennzahl lt. Studienblatt /
degree programme code as it appears on
the student record sheet:

UA 066 878

Studienrichtung lt. Studienblatt /
degree programme as it appears on
the student record sheet:

Masterstudium Verhaltens-, Neuro- und
Kognitionsbiologie

Betreut von / Supervisor:

Univ.-Prof. Dr. Thomas Hummel

Table of contents

| | |
|--|-----------|
| Abstract | 7 |
| 1. Introduction | 10 |
| 1.1 Early Life Adversities..... | 10 |
| 1.2 ELAs and neurological disorders | 11 |
| 1.3 Epigenetics..... | 12 |
| 1.4 Neuroinflammation | 14 |
| 1.5 Persistent organic pollutants | 15 |
| 1.6 Hexabromocyclododecane (HBCDD) | 17 |
| 1.7 Previous study..... | 19 |
| 1.8 Aim and hypothesis | 20 |
| 2. Material and Methods | 21 |
| 2.1 Sample collection and preparation | 21 |
| 2.1.1 Brain tissue collection | 21 |
| 2.1.2 Sample preparation: DNA, RNA and protein extraction..... | 22 |
| 2.2 Measurement of HBCDD residues in the brain by LC-MS/MS..... | 23 |
| 2.3 Neuroinflammation at PND14 – Western Blot..... | 23 |
| 2.4 Identification of 6mA as new epigenetic mark..... | 24 |
| 2.4.1 Identification of 6mA existence in the brain by LC/MS-MS | 24 |
| 2.4.2 Confirmation of 6mA existence through DotBlot | 25 |
| 2.5 Methylated DNA immunoprecipitation-sequencing | 26 |
| 2.6 Library preparation | 29 |
| 2.7 Illumina® sequencing..... | 32 |
| 2.8 Immunohistochemistry at PND270..... | 34 |
| 2.9 Statistical analysis..... | 35 |

| | |
|--|-----------|
| 3. Results | 37 |
| 3.1 Transfer of HBCDD through the placenta and blood-brain barrier | 37 |
| 3.2 Neuroinflammation at PND14 – follow of S100B marker | 37 |
| 3.3 HBCDD-induced changes in DNA methylation | 39 |
| 3.3.1 Identification of 6mA in HBCDD brains at PND14..... | 39 |
| 3.3.2 6mA validation and quantification through DotBlot | 40 |
| 3.3.3 6mA visualization through immunohistochemistry | 43 |
| 3.4 MeDIP sequencing | 45 |
| 4. Discussion | 52 |
| 5. Conclusion..... | 57 |
| 6. References | 58 |
| 7. Supplementary information | 64 |
| 8. Zusammenfassung | 75 |
| 9. Eidesstattliche Erklärung | 77 |

Abbreviations

5hmC = 5-hydroxymethylcytosine

5mC = 5-methylcytosine

6mA = *N*⁶-methyladenine

AB = antibody

AD = Alzheimer disease

ADHD = attention deficit hyperactivity disorder

AS = autism spectrum disorder

BFR = brominated flame-retardant

BPA = bisphenol A

CNS = central nervous system

CO = cytochrome oxidase

DA = dopaminergic

DS = Down syndrom

EFSA = European food safety authority

ELA = early life adversity

iNOS = inducible nitric oxide synthase

LC- MS/MS = liquid chromatography tandem mass spectrometry

PAH = polycyclic aromatic hydrocarbons

PD = Parkinson's disease

PFC = prefrontal cortex

PND = postnatal day

POP = persistent organic pollutant

RA = rheumatoid arthritis

ROS = reactive oxygen species

SES = socioeconomic status

SPRI = solid phase reversible immobilization

UNEP = United Nations environment program

WHO = World Health Organization

Danksagung

An erster Stelle, möchte ich mich bei Prof. Thomas Hummel für die Betreuung meiner Masterarbeit und die unkomplizierte Kommunikation sowie Organisation bedanken.

Anschließend möchte ich mich bei dem Luxembourg Institute of Health für die vielen Einblicke in dessen Forschung und tollen Erfahrungen bedanken. Hier sind speziell Dr. Jonathan Turner, Leiter der „Immune Endocrine and Epigenetics“ Forschungsgruppe sowie Dr. Nathalie Grova hervorzuheben. Diese gaben mir die Möglichkeit an einem spannenden Projekt mitzuarbeiten, eine Vielzahl an Techniken sowie Bereichen der epigenetischen Forschung kennenzulernen und mein Wissen darin zu vertiefen. Auch Ihre Offenheit für Diskussionen sowie regelmäßiges Feedback wusste ich sehr zu schätzen.

Ebenso möchte ich mich bei Dr. Henri Schroeder für den Zugang zu den Proben für dieses Projekt bedanken und Yordenca sowie Justine für ihre Mithilfe bei einigen Laborarbeiten erwähnen.

In diesem Kontext, möchte ich mich auch bei Sophie Mériaux, Pauline Guebels und den PhD-Studenten der Gruppe für die anfängliche Hilfe im Labor bedanken. Hier hervorzuheben ist die PhD-Studentin Sara B. Fernandes, die mir jederzeit mit Rat und Tat zur Verfügung stand. Die wertvollen Diskussionen, Erklärungen und Ideenaustausche haben mir sehr geholfen und meine Zeit im Institut extrem bereichert.

Ein wichtiger Dank gilt meinen Eltern, die mich während des gesamten Studiums immer finanziell sowie emotional unterstützt haben und ohne die ich diesen Weg nicht hätte einschlagen können.

Schlussendlich möchte ich mich noch bei meiner Schwester sowie all meinen engen Freunden bedanken die immer ein offenes Ohr hatten und mich jederzeit unterstützt haben.

Abstract

Hexabromocyclododecane (HBCDD) is a brominated flame retardant used in many manufactured materials and consisting of a technical mixture of 3 main isomers α , β and γ , where the α isomer predominates in food products and in biological compartments. Because HBCDD is found in the environmental biota, food samples and human tissues, consequences on human health are expected, especially when exposure occurs during the early developmental period.

Starting from a previous study on short-term effects, including impairments of the motor and endocrine system, caused by perinatal exposure to the environmental pollutant HBCDD [1], the current project investigated the according brain structures. As a follow-up to the previous study, the aim of this project was it to identify long-term effects of HBCDD exposure. Neuroinflammation levels were of specific interest and as pollutant exposure represents an environmental stressor, the epigenetic profile was analyzed as well.

Female Wistar rats were fed with α -HBCDD contaminated eggs during pregnancy and lactation. Since early life is a very critical period and can influence the health trajectory in later life [2], the impact of pollutant exposure needs further attention. Hence, pups were exposed to the pollutant over a period of 42 days. As the quantity of α -HBCDD was calculated according to human exposure, resulting in an administration of 66 ng/kg/day, and as 42 days in laboratory rats equal approximately 3 years in humans [3], this is considered as an early life stressor. The present study focused on the collected brains from the previous study on PND1, PND14 and PND270. Thus, the consequences of early life α -HBCDD exposure were assessed at three different timepoints, ranging from birth to adulthood. After demonstrating on PND1 brains that α -HBCDD can pass through the placenta and brain-blood-barrier, neuroinflammation levels were assessed. Significantly increased neuroinflammation in cortex was observed, encouraging the hypothesis, that pollutant exposure can impact the brain development and functioning from early stages on.

In a subsequent set of experiments, 6-methyladenine was identified as a genuine epigenetic mark. First the existence of 6-methyladenine was confirmed

through LC-MS/MS, then dynamic changes as a response to α -HBCDD exposure were analyzed through DotBlots. A clear tendency to a decrease of 6-methyladenine abundance in α -HBCDD groups compared to control groups, was seen. For instance, a decrease in male α -HBCDD rats (-30%) of 6-methyladenine abundance in the cerebellum, suggesting the ability of this contaminant to induce an early reduction of DNA methylation. A visual confirmation of 6-methyladenine occurrence in neuronal tissue of PND270 was acquired, for the first time, through immunohistochemistry assays. Finally, PND14 samples were immunoprecipitated and Illumina® sequencing was performed. This led to a listing of differential methylated regions (DMR) on every chromosome. Considerable differences on the number of DMRs were subducted, proving that the α -HBCDD exposure triggers differences in the methylation profiles. In summary, not only can α -HBCDD enter and impact the developing brain, it also clearly influences epigenetic modifications.

Keywords: early life adversity, persistent organic pollutants, HBCDD, epigenetics, neuroinflammation, 6-methyladenine

1. Introduction

1.1 Early Life Adversities

Early life adversities (ELA) have been linked to an increased risk of multiple diseases in later life. The early life period can be defined by referring to the work of Barker and colleagues dating from the 1980s. The period stretching from conception to the age of two years, also referred to as the first 1000 days, seems to play an important role in the determination of the susceptibility to various diseases over the course of time [4]. Since then, there has been considerable progress concerning the research and investigation into this correlation. Exposure to ELAs can have long-lasting effects on mental and physical health. A link can be established between adverse childhood experiences and the frequency of migraine appearance in adult life [5]. Multiple studies point out a link between poor early-life conditions and an increased risk for cardiovascular diseases [6, 7], type-2 diabetes [8], asthma [9], migraine [5], cancer [10], various autoimmune diseases [11] and mental disorders like depression for example [12, 13]. Over the years, several broad cohort studies have been conducted on this topic by different research groups and it has been demonstrated, for example, that patients who share a history of childhood abuse and neglect show a higher predisposition for autoimmune diseases like Rheumatoid arthritis [14], thereby proving that childhood traumas can have a negative impact on health even decades into adulthood. It seems that this described connection follows a dose-response trend, meaning that the risk for disease development increases proportionally to a greater ELA exposure [5]. As estimated by the World Health Organization in 2010, around 39% of the global population are exposed to at least one ELA. Interestingly, exposure to ELAs is not necessarily restricted to underdeveloped countries, as some might expect, but is distributed ubiquitously [13].

ELAs cover a whole range of different circumstances which can be classified as poor early-life conditions with negative consequences for the later life. Social ELAs include all factors which modify the social environment of a child, namely parental death or divorce, as well as separation/institutionalization or adoption. Physical, sexual and emotional abuse cover another section. From an economic

point of view, the socioeconomic status (SES), which takes into account the income as well as the educational level, can also be regarded as an ELA. For instance, a low SES can be connected to higher asthma severity [15, 16].

How important the early life environment is for the health condition in later life becomes visible by looking at the “three-hit” (figure 1) model which was first introduced by Daskalakis and colleagues in 2013. This model considers the genetic predispositions of an individual as a first hit and the early-life environment to which the individual is exposed as a second hit. The combination of those two will generate a programmed phenotype which can persist in a latent phase, without specific health issues, for decades [17]. An unknown third hit, which occurs in later life could swing the balance between resilience and vulnerability[17]. This model demonstrates how ELAs can exert their influence and how important the early-life environment is for the health trajectory of an individual (figure 1). The principle of the developmental origins of health and disease (DoHaD) underlines as well the importance of adverse circumstances during critical developmental timeframes, like pregnancy and early life, in altering various structures and creating specific phenotypes later in life [18].

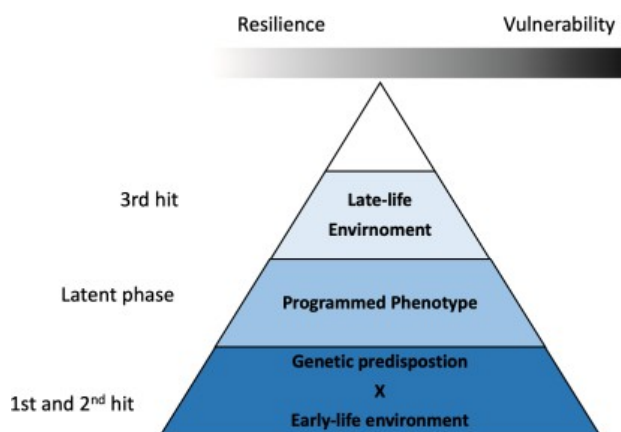


Figure 1: Three-hit model on ELA, first elaborated by Daskalakis et al. (2013)

1.2 ELAs and neurological disorders

Recent studies have focused on the immune system and how it could be affected by ELAs [19]. By investigating data from multiple human studies, it has been shown that there is a specific “ELA immune phenotype” which can have an effect

on the innate as well as the adaptive immunity [19]. This phenotype includes inflammation, accelerated immunosenescence as well as impaired cellular immunity [19].

In extension to this, the effects of ELAs on the neurological level constitute a very promising and interesting topic to look into. It is known that early life is a very critical period for brain development and maturation. While some developmental processes like neurogenesis take place even prior to birth, others like myelination continue into adulthood [20]. The brain therefore remains susceptible to environmental changes for several years after birth. Being exposed to ELAs during windows of developmental vulnerability might play a role in the lead to potential neurological disorders. As already suggested by the literature, exposure to an unspecific environmental stressor *in utero* or in early postnatal life may contribute to the emergence of later neurological disorders [21, 22].

More specifically, the early-life environment can contribute to alterations in the susceptibility of an individual to Alzheimer's disease (AD) [23]. There is evidence of the existence of early-life risk factors which can play a key role in the development of AD later in life [24]. Similar possible correlations between ELAs and later impacts on health have been demonstrated for Parkinson's disease (PD) [21, 23]. Thus, even though correlations between brain disorders and ELA's are difficult to establish with absolute certainty, it is worth having a closer look at the connection between ELAs and neurodevelopmental as well as neurodegenerative disorders, as this could contribute to the better understanding of the aetiology of such disease phenotypes. As there is a clear hint to the importance of early-life conditions for the health trajectory in later life, the identification of those factors and their impacts is necessary.

1.3 Epigenetics

Aside from genetics, the epigenome plays an important role for this topic. Neurodegenerative diseases like AD and PD are rarely exclusively triggered by genetics [21]. Such disease phenotypes often result from a combination of genetics and environmental factors [25]. As epigenetics are known to constitute the link between the environment, genes and certain phenotypes, it is a very crucial and interesting point of view.

Among the different forms of epigenetic modifications on the level of DNA, histones, chromatin and miRNAs, DNA-methylation is probably the most commonly studied one. On this note, DNA methylation is classified as a transgenerational epigenetic effect, which means that this modification is transmitted from the gametes of an exposed individual to the next generation F1. If this is the case, epigenetic modifications, which results from an environmental induction, are present in the F0 females and conserved in F1 as well as possibly also in F2, if the primordial germ cells were exposed during pregnancy. This stands in contrast to epigenetic inheritance, which takes place, when modifications are transmitted across multiple generations. If in the following generations the modification can still be observed, epigenetic heritance took place [2].

The most prevalent endogenous modification consists in a covalent binding of a methyl group to the C5 position of a cytosine in CpG dinucleotides, abbreviated as 5mC [26]. The addition of a hydroxy-methyl group is considered as hydroxyl-methylation and abbreviated as 5hmC. These epigenetic modifications can change the accessibility of the DNA and eventually lead to gene silencing by methylation of genomic regulatory regions, which can be linked to several malignant diseases [27]. There is a certain degree of plasticity in methylation levels, which can range from complete methylation of specific regions to only small methylation changes <10% which are under the influence of the environment that the organism is exposed to and related to various disease phenotypes [26]. Specific gene silencing, known as an on/off switch, is rather related to hypo- or hypermethylation whereas subtle changes in methylation are more complicated to decrypt mechanistically and are related to disease phenotypes [26]. Specific methylation patterns have been identified in neurodegenerative diseases like AD for instance [28]. As the epigenome is very sensitive to the environmental circumstances in early-life, the starting point for health issues in later life could be found in this specific period. As mentioned above, 5mC methylation changes, which are linked to later disease phenotypes, happen in a very small range and therefore it is interesting to look out for other possible methylation modifications.

Publications on another epigenetic modification, namely *N*⁶-adenin (6mA) have recently started to accumulate. The modification of 6mA is regarded as a new epigenetic mark [29], first detected in prokaryotes only, and recently also identified in several eukaryotes [30], such as mammalian cells and more specifically

mouse embryonic stem cells [30]. All this led to the discovery that 6mA is widely distributed in the human genome and that its modification is regulated by two specific enzymes, namely methyltransferase (N6AMT1) and demethylase (ALKBH1) [31]. As already mentioned, DNA coding regions can be modified and dysregulated through epigenetic modifications, which can also be the case for the genetic drivers of different cancer forms[32]. A recent study has proved that this new epigenetic mark could serve as possible therapeutic innovation for glioblastoma, as increased 6mA levels have been detected in this specific malignant brain cancer form [32]. On the other hand, this methylation is connected to different disease phenotypes; and a decrease in 6mA can for instance also promote human tumorigenesis [31]. Furthermore, 6mA shows a dynamic response to chronic stress and an increase in methylation following stress exposure, was detected in the prefrontal cortex (PFC) in mice [33]. Previous data suggests that there is a potential overlap between genes that show dynamic changes in 6mA expression and genes that are associated with neuropsychiatric disorders. This could be a hint to the importance of the changes in 6mA profiles in regard to certain disease phenotypes [33]. Taking all this information into account, it becomes clear that there are remaining gaps in the understanding of the importance and operation of this epigenetic modification. Further analysis is therefore required and should be performed while investigating changes in the epigenome due to ELAs.

1.4 Neuroinflammation

Besides causing changes in the epigenetic status, exposure to ELAs could also constitute a trigger for neuroinflammation. Basically, neuroinflammation describes the inflammatory response of the brain. The reaction can be acute as a response to injury and infection or chronic and in relation to neurodegenerative diseases [34, 35]. Microglia, which are the innate immune cells of the central nervous system (CNS), produce chemokines and cytokines in order to mediate the inflammatory response [36]. Furthermore, these mediators are important for communication with other immune cell types like astrocytes. The inflammatory reaction comes along with the generation of reactive oxygen species (ROS) and

inducible nitric oxide synthase (iNOS) [37]. The initially protective immune reaction can evolve and become toxic and chronic when it remains unresolved [34]. This reversal can be due to different circumstances. The exposure to traumatic stressors for instance can trigger a more acute neuroinflammatory profile [36]. As an example, for ELA, the exposure to air pollutants can be a possible cause for neuroinflammation. Through different pathways, exposure to pollutants can have negative effects on a developing brain [38]. In a developing organism, epithelial and blood-brain barrier are crucial and protect the growing being. However, due to air pollution exposure in early life, these barriers can be damaged and provoke an insufficient protection of the brain [39]. Once pollutants entered an organism, they will trigger an increased immune activity, including the production of cytokines. By entering and accumulating in the brain, inflammatory molecules might promote neuroinflammation [38].

A high level of neuroinflammation has been detected in rats which were exposed to diesel exhaust particles through inhalation. As a consequence, dopaminergic neurotoxicity (DA) could also be detected and hallmarks to neurodegenerative diseases like AD and PD have been identified [38, 40, 41]. Neuroinflammation can lead to the damage, or worse to the degeneration of neurons, with particular brain regions being affected at different levels [38]. Consequently, it is stated that the inflammatory mediators emerging from the neuroinflammation stimulate neurodegenerative disorders [42].

1.5 Persistent organic pollutants

As mentioned earlier, ELAs cover a broad range of different circumstances in early life. As the different forms of ELA are all interconnected, it is necessary to determine the role and importance of each [2]. The exposure to environmental pollutants in the named periods of vulnerability represents one of these adversities. Exposure to pollutants as an ELA can be an interesting research topic for several reasons. Certain studies have shown that humans can be exposed to impactful doses of pollutants during early periods of life. It has been demonstrated that polycyclic aromatic hydrocarbons (PAHs) can be transferred from mother to foetus via the placenta [43]. Additionally, a recent study investigated how mater

nal exposure to bisphenol A (BPA) can have an influence on the developing foetus. It has been proven that this pollutant is able to cross the placental barrier and a higher concentration of BPA metabolites in the cord serum than in the maternal serum was detected. This could either be explained through on-site metabolism or through poor evacuation of those metabolites in the fetoplacental compartment [44]. As the brain is very susceptible to changes during this developmental phase, exposure to pollutants may cause major damage. Early-life exposure to pollutants can also be linked to the emergence of neurodegenerative diseases later in life. Many pollutants show comparable mechanisms of toxicity, which can be based on oxidative stress. This may for example increase the concentration of protein aggregates like Tau, A β or α -syn, which will trigger neuroinflammation. Neurodegeneration can consequently be observed in specific brain regions, which are of importance in the development of AD and PD [45]. In this project, the focus will be set on persistent organic pollutants (POPs). According to the World Health Organization (WHO), POPs are carbon-based organic chemical products of global concern.

While some POPs are man-made, others form during different processes as a by-product. Dioxins, for instance, can form during combustion of waste or from burning fuels. Once released into the environment, POPs all have common characteristics. As they degrade or transform very slowly, they are persistent in the environment. Additionally, they have a high affinity to accumulate in the lipid-rich tissues of living organisms and hence increase their concentrations in ecosystems [46, 47]. As the human brain is a very lipid-rich structure, the impacts of POP exposure on this level have to be further investigated [2]. POPs can be toxic for both humans and wildlife. There are different manners in which humans can be exposed to POPs. As POPs are added to a wide variety of products, they can be found ubiquitously. Humans are principally exposed to these compounds through food and air [46]. For workers, having contact to products containing POPs on a daily basis, the cutaneous exposure is also of importance. As POPs will accumulate in living organisms, their concentration will magnify throughout the food chain. As a result, the highest concentration of POPs can be found in organisms which stand at the top of the chain [46].

Among the different categories of POPs, the project concentrated on brominated flame retardants (BFRs). According to the European food safety authority

(EFSA), BFRs are classified as mixtures of chemicals that are added to many products in order to reduce their inflammability. Mainly, they can be found in furniture, plastics and electrical articles. As BFRs are produced in extensive quantities and are persistent in the environment, possible risks for public health need to be considered. Summing up multiple studies on the risk assessment of BFRs shows that they can have a neurotoxic impact. This can include, among others, impairments of the neuromotor system, neurotransmitter system or memory formation [48].

1.6 Hexabromocyclododecane (HBCDD)

One of the most commonly used BFRs and classified as a substance of very high concern is HBCDD, which is a bromoalkene, made up of cyclododecane carrying six bromo substituents [49]. It is a chemical compound which can be found in many electronic or textile products, but especially in polystyrene isolation foam materials and therefore it is very abundant. Three isomers of HBCDD, α , β and γ , make up a mixture which can be found in various products (figure 2). In contrast to technical mixtures, where the γ -isomer is the most abundant one, the α -isomer dominates in biota [50]. Once HBCDD is released into the environment, it can bind to house dust for example [51]. The food that we eat and the water that we drink are other routes of exposure to this compound for humans. Several studies have shown that HBCDD can be detected in human breast milk as well as in serum with an approximate concentration of 1 ng/g of lipid [52, 53]. In 2011, the UNEP estimated the annual global production at approximately 28.000 tonnes per year. The daily uptake for adults ranges between 130 and 330 ng/day while that for toddlers is higher, ranging between 400 and 1500 ng/day [54, 55]. This increased exposure of toddlers is due to a higher food and water consumption per unit of body weight [2]. In 2013, HBCDD was added to the Annex A of the Stockholm Convention, whose goal it is to protect human health and environment from POPs. Compounds which are added to this list are perceived as substances of very high concern and parties must take measures to eliminate their production as well as their use. HBCDD is already known to be toxic to aquatic organisms, but the level at which it is likely to act on humans still needs to be investigated.

According to the Stockholm Convention, particular attention should be directed to the neuroendocrine and developmental toxicity of HBCDD [56].

Emerging studies show that the exposure to HBCDD can have an effect on early brain development and consequently, trigger behavioral consequences. Long-term behavioral impairments as well as attention issues were detected after prenatal exposure in rats [50]. As already mentioned, POPs can represent a risk factor for neurodegenerative diseases. In connection to this, HBCDD can trigger a disruption of the dopamine system and could therefore play a role in the development of PD. An *in vivo* study showed, that dopamine homeostasis was disrupted after exposure to HBCDD [57]. On a cellular level, HBCDD can suppress the arborization of dendrites in Purkinje cells, which demonstrates that this compound can disturb developmental processes of the brain [58]. Furthermore, a dysregulation of neural signaling can occur after HBCDD exposure. Here, specific signaling pathways like those of Ca^{2+} and Zn^{2+} will be targeted. In addition to this, HBCDD toxicity includes the formation of free radicals [59].

With regard to all this information, it seems mandatory to further investigate and clarify the impact of HBCDD neurotoxicity on humans. As mentioned above, results emerge, that show how HBCDD can act on the nervous and endocrine systems. The exact molecular mechanisms need to be revealed and the toxicity level of HBCDD for humans needs to be assessed. Only with more specific information on this pollutant, necessary protection measures could be drawn.

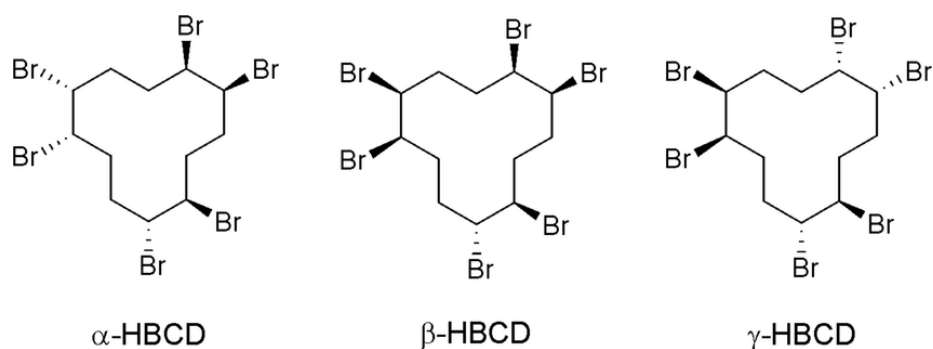


Figure 2: three most abundant isomers of HBCDD. Source: The fate of β -Hexabromocyclododecane in female C57BL/6 Mice (Sanders et al., 2013).

1.7 Previous study

This study builds up on the previous work conducted by Maurice and colleagues in 2015. The aim of this study was to define short-term neurodevelopmental effects due to an exposure to a mixture of the three HBCDD isomers during gestation and lactation. As it is still not clear, which HBCDD isomer displays which kind of toxicity, this study intended to define in the first place the neurotoxicity of α -HBCDD, as this isomer is described as the most persistent one in the environment [60]. The experiments were performed in Wistar rats, where the females were fed with α -HBCDD contaminated eggs. This food was collected as part of an experiment evaluating the carry over rate of ingested α -HBCDD in laying hens [61]. The exposure went from the day of fertilization onto the weaning day of the offspring (figure 3). Taken these two periods together, the pups were exposed to α -HBCDD for 42 days [1]. This constitutes a good model for an early life adversity as 42 days in laboratory rats are the equivalent to approximately 3 years in humans [3].

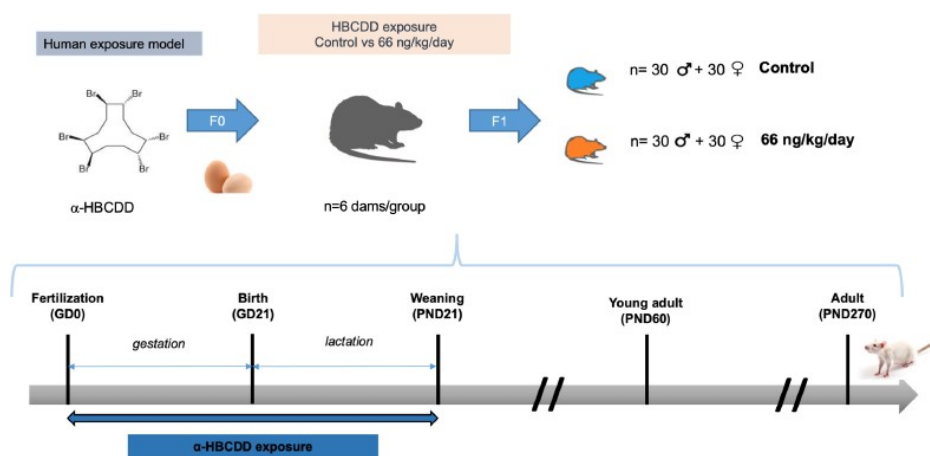


Figure 3: experimental workflow of α -HBCDD exposure model from study of Maurice et al. (2015). Pregnant Wistar rats were exposed to HBCDD contaminated eggs during pregnancy and gestation. F1 offspring was used for further behavioral and tissue analysis.

The doses of α -HBCDD, which were used to treat the rats were calculated according to a possible human exposure. Taken into account the average daily egg consumption in humans, a daily α -HBCDD intake of 2.1 to 6.3 ng/kg/day has been calculated. From this, a concentration of 66 ng/kg/day of α -HBCDD for the rats was calculated. The pups resulting from this experiment were tested at different time points of their postnatal life. The focus during early timepoints, was on possible body weight changes, impairments in the motor or sensory development as

well as locomotor activity and anxiety. Furthermore, spatial as well as short term memory have been tested and maternal behavior was observed. During adulthood, the animals of F1 were tested for social and sexual behavior and again motor coordination. These factors were tested by using different tasks like grasping reflex, locomotor coordination test, open field and elevated-plus maze for example [1]. At defined timepoints pups were sacrificed to collect the brains and eventually other organs of interest. Related to this, the activity of cytochrome oxidase (CO), a marker for the metabolic activity of cells, in the brains was analyzed. Here, significant differences were detected in regions of the auditory, visual, limbic and motor system, as well as in the brain stem and hypothalamus. Besides some differences between females and males, mostly a decrease of CO activity has been stated for the α -HBCDD group compared to the control group [62]. Overall, the results to all these tests showed impairments of the locomotor coordination in F1 pups as well as in young rats and described α -HBCDD as a possible endocrine disruptor. Later in life, the rats still showed impairments of the motor system, reduced anxiety and changes in CO activity in different brain regions for example. Overall, this study showed, that α -HBCDD can act as a developmental neurotoxicant with the specification of an exposure during gestation as well as lactation, qualifying it an early life stressor.

1.8 Aim and hypothesis

Building up on this data, this project aims to have a closer look at the developing brain, resulting from the previous study. As clear behavioral impairments have been demonstrated, it is mandatory to examine the according neuronal structures, especially the cerebellum and define possible mechanisms leading to the phenotypes. More specifically, the focus will be on the epigenetic profile, prevalent here will be the 6-methyladenine modification, as well as the levels of neuroinflammation in the exposed animals.

Taken all the previous information together, the objectives of this project were to continue the analysis of the generated brains and gather new insights on the toxicity of HBCDD from an epigenetic and neuronal point of view. PND14 represents an important timepoint for the brain development, including gliogenesis, axonal and dendritic density and consolidation of the immune system [63].

PND270, on the other hand, represents a timepoint of adolescence and tells us how the adult brain is affected by the α -HBCDD treatment and if particularities from PND14 are persistent. As this animal model is a representative human exposure model, possible extrapolations could be drawn and toxicity for humans could be evaluated. Based on this, the following hypothesis was formed. Perinatal exposure to α -HBCDD may lead to epigenetic changes of the 6mA profile in specific brain regions which are consistent over development and time. Due to the early life pollutant exposure, neuroinflammation might be upregulated and could play a key role in the aetiology of certain neurodevelopmental or neurodegenerative disease phenotypes. Modified levels of neuroinflammation and early dynamic changes in DNA methylation could be part of the mechanisms which triggered behavioral impairments in the exposed animals and explain the operation mode of HBCDD.

2. Material and Methods

2.1 Sample collection and preparation

2.1.1 Brain tissue collection

The brains used for this project were collected from pups of the F1 generation whose mothers (Wistar rats, n= 6) were daily exposed to a concentration of 66 ng/kg of α -HBCDD through contaminated eggs. The control group (n= 6 dams) was fed with commercial non-contaminated eggs. Therefore, the pups were exposed during both pregnancy and lactation period [1]. Within the wider framework of this experiment, pups were sacrificed at PND1, PND14, PND270, where brains were collected and stored at -80° before use.

- At PND1, the brains of 2 exposed and 2 control pups were used to evaluate the internal dose of the 3 HBCDD isomers.

- At PND14, 9 animals were randomly and accordingly to the treatment selected from 6 litters to constitute the control group (4 females and 5 males) and the α -HBCDD group (5 females and 4 males). For further analysis, regional dissection was performed and frontal cortex, hippocampus, cerebellum and brain-stem were isolated.

- At PND270, 10 animals were randomly selected over the 6 respective litters to constitute the control group (6 females and 4 males) and the α -HBCDD

group (5 females and 5 males). The brains collected from these individuals were used to carry out histological slices of 20 μm in a frontal plan (figure 4). Eight series, with 10 cutting levels were prepared for every brain. Six slices were put on one microscopic glass slide. One series of slices was initially used for the analysis of cytochrome oxidase activity. Since a positive relationship was demonstrated between enzymatic and neuronal activity, CO was used as a marker of metabolic activity in neurons [62, 64].

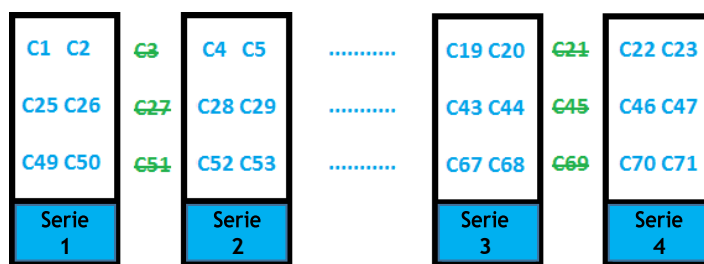


Figure 4: scheme of PND270 brain slice organization on microscopic glass slides; in total 8 series with 10 cutting levels (C) were prepared

2.1.2 Sample preparation: DNA, RNA and protein extraction

DNA, RNA and proteins were extracted from PND14 brains by using the Qiagen AllPrep DNA/RNA/Protein Mini Kit (ref 80004, Netherlands) according to the manufacturer's recommendations. Around 30 mg of starting material were necessary to perform simultaneous purification of the three products. As all the PND270 brain samples were initially conditioned under histological slices to perform immunochemistry analysis, the DNA extraction was only conducted on cerebellar tissue which was extracted out of the PND270 brain slices by using the Qiagen DNA Micro Kit (ref 56304, Netherlands). This kit offers the possibility to work on small quantities of starting material (< 10 mg). The choice of the cerebellum as a first region of interest at PND270, was defined based on the behavioral results previously obtained by the research group in charge of the animal experiment (Dr. H Schroeder, Calbinotox, France), as well as the results obtained on the measurements of 6mA abundance in the PND14 brains. Afterwards, 2 μL of each sample were used to determine the concentration in DNA, RNA or proteins, by using the Thermo Scientific™ NanoDrop™ spectrophotometer. All the samples were stored at -80°C .

2.2 Measurement of HBCDD residues in the brain by LC-MS/MS

Some pups were sacrificed on PND1 to prove that the pollutant can be detected in different tissues, including the brain, and confirming that it is able to pass through the mother to the offspring, making it an important environmental stressor.

The concentration levels of α -, β - and γ -HBCDD in the brain were determined using a validated mass spectrometric method already used to assess human internal exposure to POPs including HBCDD by the LABERCA (Oniris, Nantes, France) [65, 66]. The refined characterization of the related +/- enantiomers was performed according to a complementary characterization of the prepared sample extracts on a dedicated chiral chromatographic system. The procedure included the addition of ^{13}C -labelled congeners to every sample in order to quantify along the isotopic dilution method. After a liquid/liquid pentane extraction, the fat content of the extracts was defined (gravimetric method) and samples were reconstituted in hexane [66]. Then, three successive acid silica, florisil, and celite/carbon columns were applied for lipid removal, fractionation and further purification, respectively. Quantification of HBCDD isomers was performed through a liquid chromatography coupled to mass spectrometry (LC-MS/MS), this through the use of a triple quadrupole instrument (Agilent 6410) [67] with two diagnostic signals for detection and unambiguous identification.

2.3 Neuroinflammation at PND14 – Western Blot

Proteins which were extracted from the different brain regions were used to define levels of neuroinflammation in α -HBCDD and control groups. For this, specific markers can be used. Here S100B, which is a calcium-binding protein, was investigated. As it is synthesized in astrocytes it can be used as a parameter of glial activation. Increased S100B levels have been associated with neurodegenerative and neuroinflammatory diseases and it has been hypothesized that it can be involved in PD [68].

For immunoblot experiences, brain protein extracts had to be lysed with a buffer (RIPA lysis buffer, Millipore Corporation). For a better functioning, phosphatase and protease inhibitor cocktails were added (Roche, France) [69]. Protein concentration was then defined by using the BCA protein assay kit (Thermo Fisher, France).

After proteins (20 µg) were electrophoresed on a 15% sodium dodecyl sulfate polyacrylamide gel (Bio-Rad), they were transferred to a nitrocellulose membrane (GE, healthcare, Saclay, France) [69]. Further treatment included a 2h blocking buffer (20 mM Tris-HCL, pH 8.0, 500mM NaCl, 0.1% tween 20, 5% skimmed milk) period at room temperature. This was followed by an overnight incubation at 4°C with the primary antibody: mouse monoclonal anti-S100 antibody (1:2000, Thermo Fisher, MAS-12969) or rabbit monoclonal anti β actin antibody (1:4000, Sigma Aldrich, A2103). On the next day, after three washes with blocking buffer, membranes were incubated with horseradish peroxidase-conjugated anti-mouse or anti-rabbit IgG secondary antibody. A chemiluminescence kit (GE, Healthcare, France) was used to prove immunoreactivity [69]. Images from Western Blot experiments were acquired by the means of the Image Lab software on a ChemiDoc instrument (Biorad, France).

2.4 Identification of 6mA as new epigenetic mark

2.4.1 Identification of 6mA existence in the brain by LC/MS-MS

In order to identify and confirm the occurrence of 6mA in the PND14 brains, some representative samples of each condition were analyzed with LC-MS/MS.

Afterwards, the existence was validated and further investigated with the DotBlot technique.

A liquid chromatography tandem mass spectrometry (LC-MS/MS) method was optimized for the identification and quantification of adenine (A) and N6-Methyl-adenine (6mA) using an ACQUITY UPLC coupled to a Xevo TQ-XS mass spectrometer in collaboration with Dr R. Duca and his collaborator (Centre for Environment and Health, KU Leuven, Leuven, Belgium). After DNA had been isolated, 1 µg was enzymatically hydrolyzed, resulting in individual deoxyribonucleosides [70]. The digest mix included alkaline phosphatase, phosphodiesterase I and Benzonase® Nuclease to Tris-HCl buffer. Extracted DNA was supplemented with [¹⁵N₃]-2'-deoxycytidine, which functioned as an internal standard. Then it was ready to be dried and hydrolyzed, by using 10 µl digest mix, at 37°C for 8 hours [70]. After hydrolysis, the samples were diluted with water, filtered using an Amicon Ultra-0.5 Centrifugal Filter device and re-suspended in a solution of ACN:H₂O (70:30, v/v).

A 10 μ L aliquot was injected on a hydrophilic interaction liquid chromatography (HILIC) column (ACQUITY UPLC® BEH Amide columns 1.7 μ m, 2.1 x 50 mm), which had a temperature of 40°C. The mobile phase of the chromatography, which was necessary for the separation, was a mix of 1mM Ammonium Fluoride (A) and acetonitrile (B) [71]. During the setups, the flow rate was defined to 0.4 mL/min. Electrospray ionization (ESI) in a positive mode were used for the analyses and compounds were identified with multiple reactions monitoring (MRM). Here, argon was used as the collision gas [71]. MS/MS parameters for the specific detection by MRM are detailed in table 1.

Table 1: MS/MS parameters for specific detection by MRM for each target compound

| Compounds | Ionization mode | Transitions (m/z) | Collision energy (eV) | Cone (V) |
|------------------------------|-----------------|-----------------------|-----------------------|----------|
| [15N3]-2'-deoxycytidine (IS) | ESI+ | 231 \rightarrow 115 | 15 | 12 |
| adenosine | ESI+ | 268 \rightarrow 135 | 18 | 26 |
| | ESI+ | 268 \rightarrow 119 | 42 | 26 |
| 6-methyl-adenosine | ESI+ | 282 \rightarrow 149 | 14 | 2 |
| | ESI+ | 282 \rightarrow 133 | 40 | 2 |

Detection with tandem mass spectrometry allows great selectivity. Not only, will compounds be identified but also presence can be confirmed with MRM transitions. Those are even more compound-specific than a single ion monitoring mode [72]. Regarding the specificity of the method presented here, in addition to the transition of quantification, an additional confirmation transition was used to ensure the presence of each target compound (table 1). To confirm the presence of target compound, the ratio “quantification transition” to “confirmation transition” had to be below 20% different from the ratio obtained with standard compounds.

2.4.2 Confirmation of 6mA existence through DotBlot

The DotBlot technique was used as supplementary assay to identify the 6mA as a new epigenetic mark. First of all, it allows detecting whether this methylation occurs in the according brain region and also whether exposure to α -HBCDD can induce dynamic changes in the levels of 6mA. The method was adapted from the one of Wu et al [30]. After prior optimization, a quantity of 50 ng of DNA was selected. All the dilutions of the DNA samples according to this concentration

were prepared with UltraPure™ DNase/RNase-Free Distilled Water (Invitrogen) in a PCR plate. Before starting, membrane design was performed. Normally, all the DNA samples from the control group were placed in the same row and all the DNA samples from the α -HBCDD group below, or vice-versa.

The first step of the method consisted in the denaturation of the DNA samples at 95°C for 5 minutes, followed by a cool down on ice. The neutralization step was achieved with 10% vol of 6.6 M ammonium acetate by what DNA was precipitated and concentrated. The samples were then spotted on a nitrocellulose membrane and air-dried until the spots were no longer visible. Once the membranes were dry, the DNA was fixed to the membrane by UV-crosslinking for 1,5 min. After a 2 h incubation at room temperature with blocking buffer (1% BSA, 5% milk, PBST 0,1 %), membranes were incubated with the 6mA primary antibody (Synaptic Systems, ref 202 003, Germany, 1:1000) overnight at 4°C. On the next day, the membranes were washed 3 times for 10 min each with PBST 0.1 %, followed by an incubation with the secondary anti-rabbit IgG AB (Synaptic systems, Germany, 1:5000) for 1h at room temperature. After additional 3 washes with PBST 0.1 %, the signals of the membranes were revealed with ECL Western Blotting Reagent (PerkinElmer, Germany). After 5 minutes incubation away from light, the signal was detected in the ECL Chemocam Imager (Intas, Germany).

Both, α -HBCDD and control samples of each brain region investigated at PND14 and PND270 were performed on the same membrane. All membranes were done in triplicates. The obtained images were quantified with ImageJ and the raw data was used to evaluate the signal intensity of 6mA.

2.5 Methylated DNA immunoprecipitation-sequencing

MeDIP-sequencing was performed on the four brain regions collected on both exposed and control pups at PND14, to evaluate changes in the complete methylation profile. Methylated DNA immunoprecipitation (MeDIP) can be used to analyze specific epigenetic modifications. *Via* immunoprecipitation with specific antibodies, methylated DNA can be isolated from genomic DNA. Technically, after the DNA is fragmented, an incubation with according antibodies will precipitate the methylated DNA. After purification of the DNA and library preparation samples will be sequenced. In this case Illumina® sequencing was used. Since it was

only possible to have a limited number of samples sequenced, the PND14 samples were pooled along the following scheme (table 2), resulting in a total of 16 pools. The pools were characterized by brain region, sex and treatment as described below.

Table 2: PND14 DNA pools for MeDIP protocol. Samples were pooled along brain region, sex and treatment (α -HBCDD vs control). Every pool consisted of a total of 5 μ g of DNA.

| MeDIP samples | Sample type | Animals | Treatment |
|---------------|-------------|-----------|-------------------------|
| Pool 1 | Cortex | 5 females | α -HBCDD females |
| Pool 2 | Cerebellum | 5 females | α -HBCDD females |
| Pool 3 | Brainstem | 5 females | α -HBCDD females |
| Pool 4 | Hippocampus | 5 females | α -HBCDD females |
| Pool 5 | Cortex | 4 females | Control females |
| Pool 6 | Cerebellum | 4 females | Control females |
| Pool 7 | Brainstem | 4 females | Control females |
| Pool 8 | Hippocampus | 4 females | Control females |
| Pool 9 | Cortex | 4 males | α -HBCDD males |
| Pool 10 | Cerebellum | 4 males | α -HBCDD males |
| Pool 11 | Brainstem | 4 males | α -HBCDD males |
| Pool 12 | Hippocampus | 4 males | α -HBCDD males |
| Pool 13 | Cortex | 5 males | Control males |
| Pool 14 | Cerebellum | 5 males | Control males |
| Pool 15 | Brainstem | 5 males | Control males |
| Pool 16 | Hippocampus | 5 males | Control males |

As the DNA needed to be fragmented for the MeDIP, for every pool, a quantity of 5 μ g was prepared in a total volume of 100 μ L. For this, 1 μ g of each sample (n=5), that made up one pool, was used. If needed, the volume was filled up with TE buffer to 100 μ L. Afterwards, the pools were sonicated in the Bioruptor UCD-200 (Diagenode) for 14 minutes of 30"/30" ON/OFF cycles with the output selector switch on High and this at 4°C. After sonication, 1 μ L of each sample was tested on the 2100 Bioanalyzer (Agilent, DNA High sensitivity chip), an automated electrophoresis tool used to: i) control the sample quality, ii) verify that the DNA was correctly fragmented and ranged between 200 and 700 bp. After the design of the KingFisher plate, the MeDIP protocol could be started with the first step corresponding to the bead preparation (example table 3). 8 pools were treated

simultaneously by plate. Non-specific rat DNA, provided by Sara B. Fernandes (PhD student of the group), was used in the protocol as negative controls.

Table 3: Example of plate design for the MeDIP protocol. 8 PND14 DNA pools were run on 1 plate; on position 9 and 10 were negative controls from non-specific rat DNA.

| 1 | 2 | 3 | 4 | 5 | 6 | 7 | 8 | 9 | 10 |
|--------|--------|--------|--------|--------|--------|--------|--------|---------------------------------|------------------------|
| Pool 1 | Pool 2 | Pool 3 | Pool 4 | Pool 5 | Pool 6 | Pool 7 | Pool 8 | @GR control Ab (H300X), rat DNA | No Ab control, rat DNA |

The wells of the first KingFischer plate were filled consecutively with 50 μ L of Dynabeads™ M-280 Sheep Anti-Rabbit IgG (Thermo Fisher Scientific, ref 11203D), blocking solution 1 (1x PBS, 0,5% BSA), the according antibody (AB) for 6mA (Synaptic Systems, ref 202 003) and negative controls Rabbit anti-GR (Santa Cruz biotechnologies, ref H300X). Following wells were filled with blocking solution 2 (1x PBS, 0,05% BSA) and blocking solution 3 (1x PBS, 3% BSA). The detailed protocols for the KingFischer plates 1 and 2 are listed in the supplementary information. This supplemental data describes, how in plate 1 the beads are washed, coated with the AB of interest and blocked to avoid unspecific binding of DNA. The plate 1 was then placed in the KingFischer machine at 4°C for approximately 7 hours.

On the second step, spike-in oligos were added to the sonicated DNA and this mixture was then denatured at 95°C, followed by cooling down on ice. At this stage, the wells of the KingFischer plate 2 were ready to be filled. This included 2x IP buffer (0,05% Triton, 50 μ g/mL yeast tRNA in 1x PBS) with blocking solution 2 and 80 μ L of the denaturized DNA. Following steps included IP wash buffer (0,025% Triton in 1x PBS) and IP stringent wash buffer (0,050% Triton in 1x PBS). The protocol for the plate 2 was running on the KingFischer machine for approximately 17 hours. On day 2, the elution step was carried out.

At the end of the second run in the KingFischer machine, the bead-antibody-DNA complexes were released into the digestion buffer (50mM Tris, 10mM EDTA,

0,5% SDS, pH8). Protein kinase K was added and the beads were put at 50°C for 3h with agitation, to elute the DNA from the bead-antibody complexes. The final step of the MeDIP protocol was the DNA purification, which was performed through magnetic beads (Sera-mag SpeedBeads, Fisher Scientific, ref 11548692). The samples were put on a magnetic rack and the liquid containing the immunoprecipitated DNA was transferred to new tubes and incubated with 1.8x volume of beads where the DNA binds to. Back on the magnetic rack, the supernatant was discarded and the beads were washed twice with 70% ethanol. Once the bead pellet was dried, it was resuspended in low EDTA TE buffer, put back on the magnetic rack and the purified DNA was collected.

2.6 Library preparation

Before proceeding with the Illumina® sequencing, libraries of the immunoprecipitated DNA needed to be prepared. For this, the Accel-NGS® 1S Plus DNA Library Kit was used. Library preparation describes the generation of DNA fragments which are ligated with specialized adapters to both fragments ends of single-stranded DNA. The protocol includes 8 steps, namely: Denaturation, adaptase step, extension step, post-extension SPRIselect step, ligation step, SPRIselect step, indexing PCR and SPRIselect step (figure 5). A detailed protocol can be found in the supplementary information.

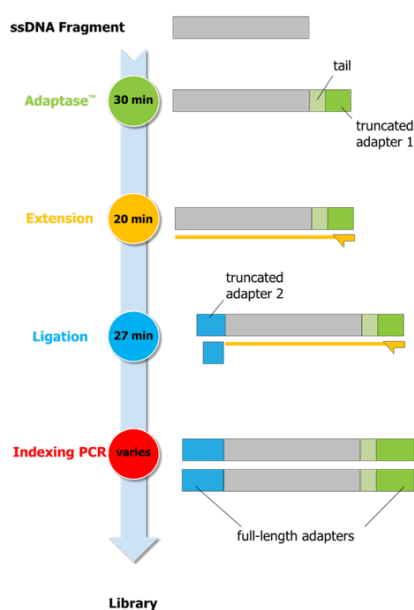


Figure 5: protocol overview for library preparation. Source: Accel-NGS® 1S Plus DNA Library Kit for Illumina® Platforms

During denaturation, the fragmented DNA was incubated for 2 min at 95°C in a thermocycler. Next was the adaptase step, during which the ligations of the first truncated adapters to 3' ends took place. To facilitate the ligation of the next adaptors, the extension step synthesized a strand which guided the following steps. This strand was not sequenced later on. The extension was followed by a bead-based SPRIselect clean-up. To add a brief explanation, the SPRIselect is used to make a size selection of DNA fragments during library preparation and fragments smaller than 200 bp are excluded. This is necessary to generate a total of fragments around 350 bp, which are needed for the later sequencing protocol. In this protocol, a left side size selection has been performed, which means that an increase in the ratio between SPRIselect beads volume to sample volume will increase the efficiency of binding smaller fragments. So basically, an increase in the ratio between SPRIselect beads volume and sample volume will increase the concentration of polyethylene glycol and smaller fragments will be fixed. On the other way around, if the ratio between SPRIselect volume and sample volume is smaller, bigger fragments will be selected. To recover fragments around 200 bp, the ratio was set to 0.8 during library preparation. The chemical properties and polarity of the DNA, make it possible that it can aggregate and precipitate onto the magnetic beads. Once the supernatant is taken away, the DNA fragments can be washed, eluted and the selected sizes can be retrieved (figure 6). SPRIselect steps were introduced on multiple points during the protocol, to make sure, that the libraries have the right sizes and are as clean as possible and free of interfering enzymes for example. After the clean-up, the second adaptor was added to the 5' ends and the samples undergo another SPRIselect step.

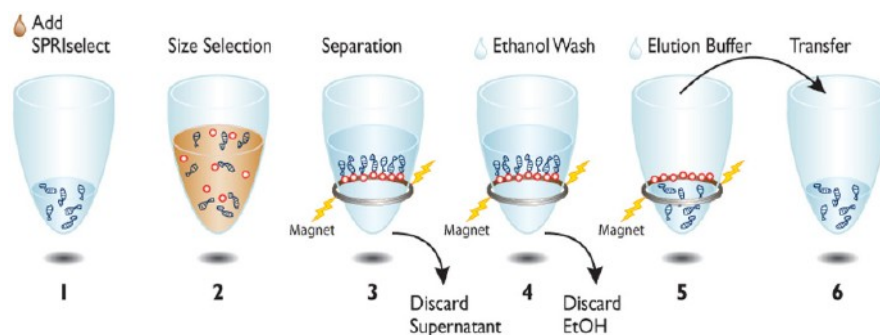


Figure 6: left side size selection of the immunoprecipitated DNA with SPRIselect beads.
Source: SPRIselect User Guide

Upcoming was the indexing PCR, which is a crucial point of the protocol. It amplified the libraries and added the variable indices to them, which were used to label the samples and distinguish them in the later sequencing. The following indices have been used for the PND14 brain samples (named now library 1-16, in accordance to the naming of the pools before).

Table 4: Indices used during indexing PCR of library preparation to label the samples for later sequencing

| Library | Index number | Index sequence |
|----------------|---------------------|-----------------------|
| Library 1 | I18 | GTCCGC(A) |
| Library 2 | I2 | CGATGT(A) |
| Library 3 | I4 | TGACCA(A) |
| Library 4 | I5 | ACAGTG(A) |
| Library 5 | I6 | GCCAAT(A) |
| Library 6 | I7 | CAGATC(A) |
| Library 7 | I12 | CTTGTA(A) |
| Library 8 | I13 | AGTCAA(C) |
| Library 10 | I19 | GTGAAA(C) |
| Library 11 | I18 | GTCCGC(A) |
| Library 12 | I16 | CCGTCC(C) |
| Library 13 | I15 | ATGTCA(G) |
| Library 14 | I5 | ACAGTG(A) |
| Library 15 | I6 | GCCAAT(A) |
| Library 16 | I4 | TGACCA(A) |

Finally, two SPRIselect clean-ups were performed to ensure a high quality. Final libraries were tested on the 2100 Bioanalyzer to control the size distribution of the adapter-ligated fragment libraries as well as the quality and quantification after the PCR. The Bioanalyzer data (concentration and fragment size) were then used for the calculation and preparation of the samples before sequencing. To add another quantification method, the libraries were quantified with the dsQubit assay, which uses specific dyes that emit fluorescence when bound to DNA and is more sensitive than UV absorbance.

2.7 Illumina® sequencing

For this project, the Illumina® dye sequencing method was used, and previous samples were prepared for this purpose. As for every DNA sequencing method, also this one aims to determine the series of base pairs. Here, the focus is on the use of dye-terminators which make it possible to identify every single base [73]. The three main steps of this technique are amplification on a solid surface, sequencing and analysis (figure 7) [74]. The adapters and indices, which are added during library preparation, will be used as reference points during these steps. The libraries are then loaded onto a flow cell which contains oligonucleotides. Four libraries can be run on one flow cell. The template fragments will hybridize to them and bind to the flow cell. Following this, the cluster generation will start. This is a solid phase, which will amplify the DNA and create approximately thousands of copies of every template. The amplification clusters are formed through bridge amplification. The fixed templates are used to create the complementary strands (reverse strand) by the action of the DNA polymerase. As the reverse strand carries an adapter, it will bend over and bind to an oligonucleotide, which is fixed to the flow cell, and presents the complementary sequence. Resulting from this is a double stranded DNA, which is separated again, so that the strands can bind to the according oligos. The dNTPs which are introduced for amplification carry reversible 3' terminators as well as fluorescent tags. This implies, that the polymerase can only add one single base to a growing DNA copy strand at a time. The fluorescent labels are recorded by a camera after every round of synthesis. The wavelength of the emission of the tags are used to determine which base is added to the strand. After the four bases have been added in separate cycles, the images can be recorded and the terminators and tags can be removed.

The output data is aligned to a reference genome, in this case the rat genome, by using a specialized software. After analysis, differences between the reference and the newly generated sequences can be determined.

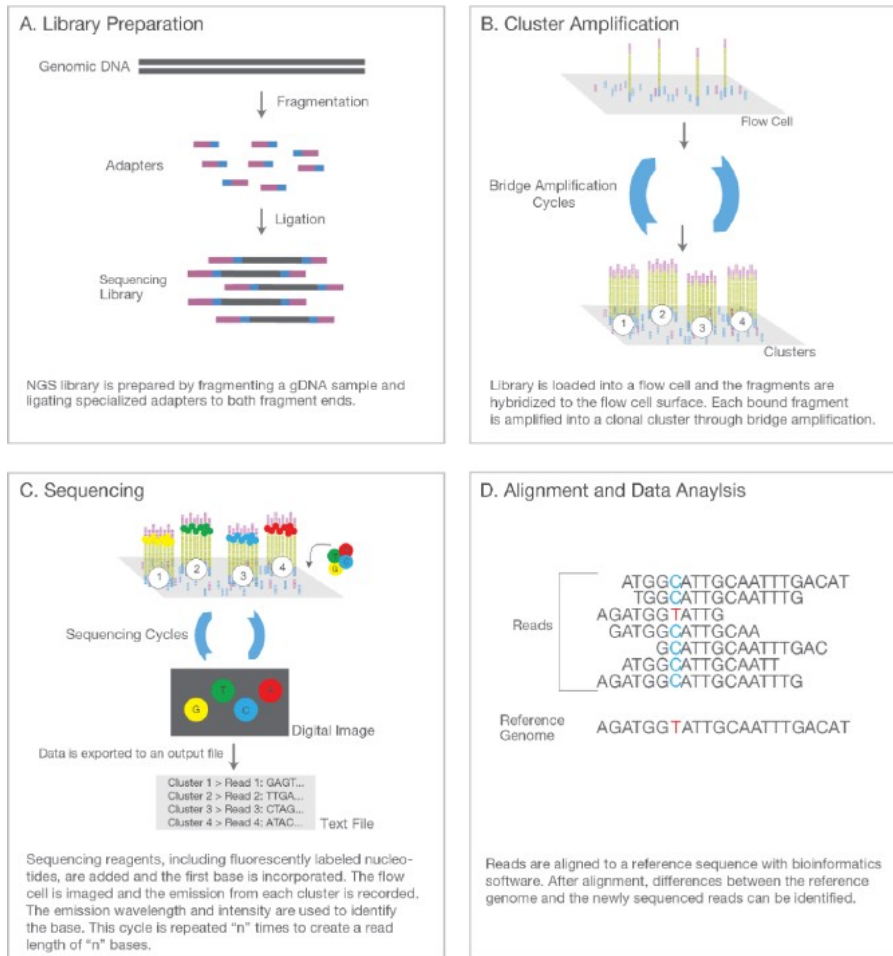


Figure 7: Illumina® sequencing overview – library preparation, cluster generation, sequencing and data analysis. Source: Illumina – An introduction to next-generation sequencing technology.

The Illumina sequencing of the PND14 samples has been done in cooperation with the LuxGen platform, which constitutes the national sequencing center. Libraries needed to be normalized to 15 nM and the following formula was used to prepare the samples.

$$C(nM) = \frac{C(\eta g/\mu L) * 10^6}{((frgmtsize * 607,1) + 157,9)}$$

Figure 8: formula to calculate the nano molarity of the libraries

Due to measuring issues with the dsQubit assay, the concentrations (ng/μL) and fragment sizes were taken from the Bioanalyzer data. Nano molarity could be defined and the required amount of library and buffer was calculated. A total volume of 15 μL of every library at a concentration of 15 nM were prepared in a PCR plate, in a Tris-HCL 0,1% Tween buffer (table 5).

Table 5: values to calculate nano molarity of the libraries and amount of library and buffer used to prepare the samples for sequencing at LuxGen

| Sample | Conc. (ng/ μ L) | Frag. size (bp) | nM | Library (μ L) | Buffer (μ L) | Total volume (μ L) |
|--------|---------------------|-----------------|--------|--------------------|-------------------|-------------------------|
| Lib 1 | 28.81 | 497 | 95.43 | 7.86 | 42.14 | 50 |
| Lib 2 | 22.29 | 506 | 72.52 | 10.34 | 39.66 | 50 |
| Lib 3 | 21.17 | 499 | 79.74 | 9.41 | 40.59 | 50 |
| Lib 4 | 30.24 | 254 | 110.01 | 6.82 | 43.18 | 50 |
| Lib 5 | 28.66 | 510 | 92.52 | 8.11 | 41.89 | 50 |
| Lib 6 | 26.58 | 453 | 96.59 | 7.76 | 42.24 | 50 |
| Lib 7 | 24.33 | 549 | 72.96 | 10.28 | 39.72 | 50 |
| Lib 8 | 17.63 | 457 | 63.51 | 11.81 | 38.19 | 50 |
| Lib 10 | 18.38 | 515 | 58.76 | 12.76 | 37.24 | 50 |
| Lib 11 | 9.84 | 588 | 27.55 | 27.22 | 22.78 | 50 |
| Lib 12 | 27.36 | 447 | 100.76 | 7.44 | 42.56 | 50 |
| Lib 13 | 15.38 | 513 | 49.04 | 12.24 | 27.76 | 40 |
| Lib 14 | 22.29 | 507 | 72.38 | 10.36 | 39.64 | 50 |
| Lib 15 | 21.69 | 565 | 63.20 | 11.87 | 38.13 | 50 |
| Lib 16 | 11.35 | 490 | 38.13 | 15.73 | 24.17 | 40 |

2.8 Immunohistochemistry at PND270

Immunohistochemistry assays were performed to i) firstly identify and prove the existence of 6mA in brain tissues and ii) secondly, to highlight possible differences in 6mA concentration between the α -HBCDD and the control groups. These analyses were set up firstly on the cerebellum, based on the previous results obtained on behavior, CO analysis, as well as preliminary results obtained at PND14. Brain tissue collected at PND 270 was previously sliced at 20 μ m and coated on slides to carry out CO and acetylcholinesterase analysis. As the slides were stored at -80°C, they were brought to room temperature for 10 min and then rinsed with PBS 1x for 5 min. After that, they were put in a glass strainer and rehydrated with rehydration buffer (PBS1X, Triton-X 0.3%) for 10 min. This also contributed to permeabilization of the slices. The slides were then incubated with 2M HCl for 45 min, followed by 20 min in 0.1 Tris-HCl. The slides were incubated in blocking buffer (PBS1X, BSA 1%, Triton-X 0.3%, RNase A) for 1h. After the blocking step, the slides were washed 3 times with PBS 1X, 5 min each and then

incubated with the primary AB. For the 6mA detection, the primary AB (6mA, Synaptic Systems, ref 202-003) was used at a dilution of 1:500 and put on the slides for approximately 1h at room temperature. Following, was another round of PBS1 X washes, before the secondary AB was applied. As the primary AB was a polyclonal rabbit AB, this has to be taken into consideration when choosing the secondary fluorescent AB. For this project, the secondary AB was Alexa Fluor 488 (ab150077, Abcam) at a dilution of 1:2000. The slides were incubated for 1h at room temperature and kept away from light, as all the following steps were. After incubation, the slides were washed again, to remove all leftover AB. Finally, the samples were mounted with anti-fade mounting medium which contained DAPI (Thermo Fisher) and covered with a cover slip. DAPI stains the nuclei and therefore helps to locate the methylation in the cell. Once the slides were dry, they were analyzed by using the fluorescence microscope from Zeiss. The different channels (DAPI, AF 488) needed to be set up and different objectives were used to acquire different images. If a whole cerebellum picture wanted to be taken, multiple focus points were set, to assure the sharpness of the picture. The immunofluorescent pictures were not used for quantification but as a means of methylation profile confirmation in the cerebellum. To represent the α -HBCDD and control group, two males and 2 females were taken out of each group to perform this protocol and generate representative pictures.

2.9 Statistical analysis

For each variable measured in the present study, a Levene test was firstly performed to test the homogeneity of variances. Further statistical analysis was performed with a general linear model (GLM), which was possible because homogeneity of variance was assumed for almost all variables. In the GLM, the litter served as a confounding variable [1]. Values for within-litter variability had to be adjusted, therefore post-hoc comparisons were not applicable. The number of animals that completed the test was evaluated with a Pearson chi-square test. All results, except concentration and identification levels of HBCDD isomers in brain tissue, have been expressed as median and quartiles. This was necessary to correctly represent the distribution of each variable, specifically for those which were not normally distributed [1].

Significance was set at $p < 0.05$. All statistical analyses were carried out using R software (version 3.2.3).

3. Results

3.1 Transfer of HBCDD through the placenta and blood-brain barrier

To start off, brains of pups that were sacrificed at PND1 were used to determine the concentration of the different HBCDD isomers in the tissue. By using this early timepoint, it was possible to prove that the pollutant can be transferred from the mother to the pups and also pass the blood-brain barrier. Quantification of HBCDD isomers was performed through a liquid chromatography coupled to mass spectrometry (LC-MS/MS), this through the use of a triple quadrupole instrument (Agilent 6410) [67] with two diagnostic signals for detection and unambiguous identification.

As regards with the concentration levels of HBCDD in the brains of pups at PND1, the analysis carried out by LC-MS/MS clearly demonstrated the presence of the three isomers of HBCDD (figure 9). Even though, only two animals per group (exposed *versus* control) were available, detectable levels of the 3 isomers were found in both controls and exposed group.

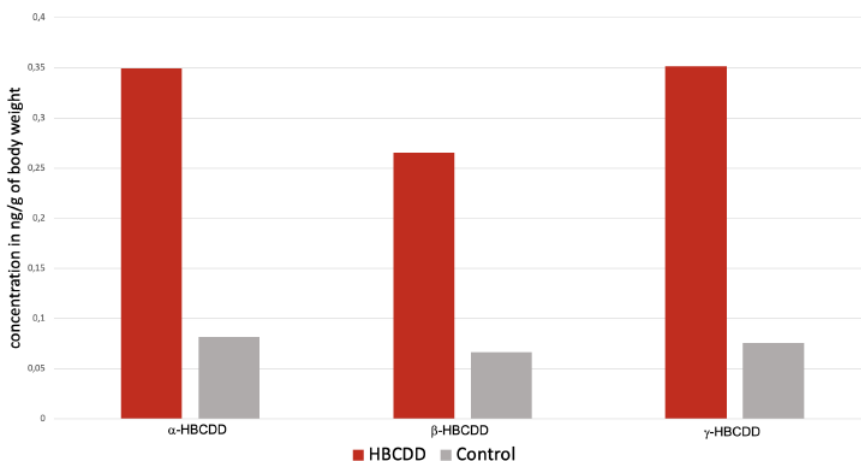


Figure 9: Concentration of HBCDD isomers in the brains of pups at PND1; analysis by LC-MS/MS. Results are represented by the mean of the values (HBCDD n=2, control n=2)

3.2 Neuroinflammation at PND14 – follow of S100B marker

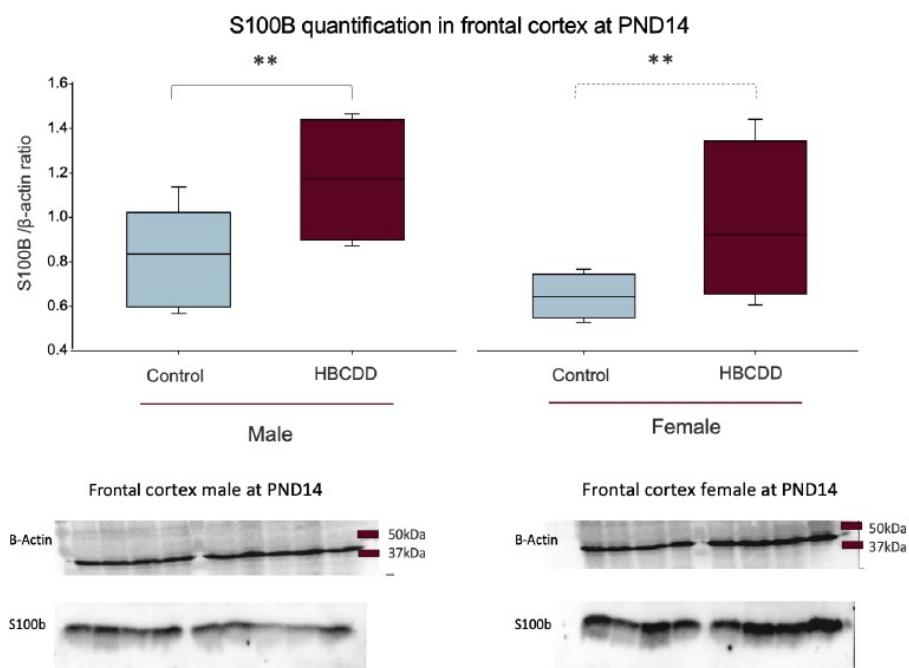
At PND14, brain samples were analyzed in order to define if an exposure to α -HBCDD during the gestation and the lactation is able to induce neuroinflammation at an early stage of life. Proteins which were extracted from the different brain

regions were used to define levels of neuroinflammation in α -HBCDD and control groups.

As S100B, which is a calcium-binding protein, is synthesized predominantly in astroglia cells of the CNS, and also to a lesser extent, in neurons, microglia, and oligodendrocytes, it was chosen as a marker of neuroinflammation in the present study. S100B is the major S100 protein recovered in brain, and under normal physiological states it represents in approximately 0.5% of all brain proteins.

In various neuropathological conditions, that might be induced by environmental stressors like trauma, infection or psychiatric conditions, S100B levels can vary [75]. Distribution within the brain can diverge and therefore function as an indicator for neuroinflammation. In this context, S100B is also often used as a marker for brain injury [75].

Western blot analysis of S100B showed that at PND 14, the concentration of this protein was significantly higher in the cortex of α -HBCDD exposed animals compared to the control groups in both sex ($p < 0.01$) (figure 10). HBCDD-induced changes in S100B protein levels were dependent on the factor sex ($F = 3.654$, $p < 0.05$).



*Figure 10: Effects of early α -HBCDD exposure on level of S100B expression in the frontal cortex. As described in Material and Methods, immunoblotting was performed to assess normalized protein expression levels of S100B. For these experiments, β -actin was the loading control [76]. Shown results are represented as quartiles and median. A statistical GLM was performed for the main effect of α -HBCDD exposure between females (dotted line) and males (full line) of two groups (** $p < 0.01$). Any kind of interactions are stated in the according text [1].*

In the cerebellum, no significant difference was noticed between both groups and between males and females in the protein expression levels for S100B (figure 11). Significant interaction between HBCDD and sex was observed ($F= 0.1325$) as well.

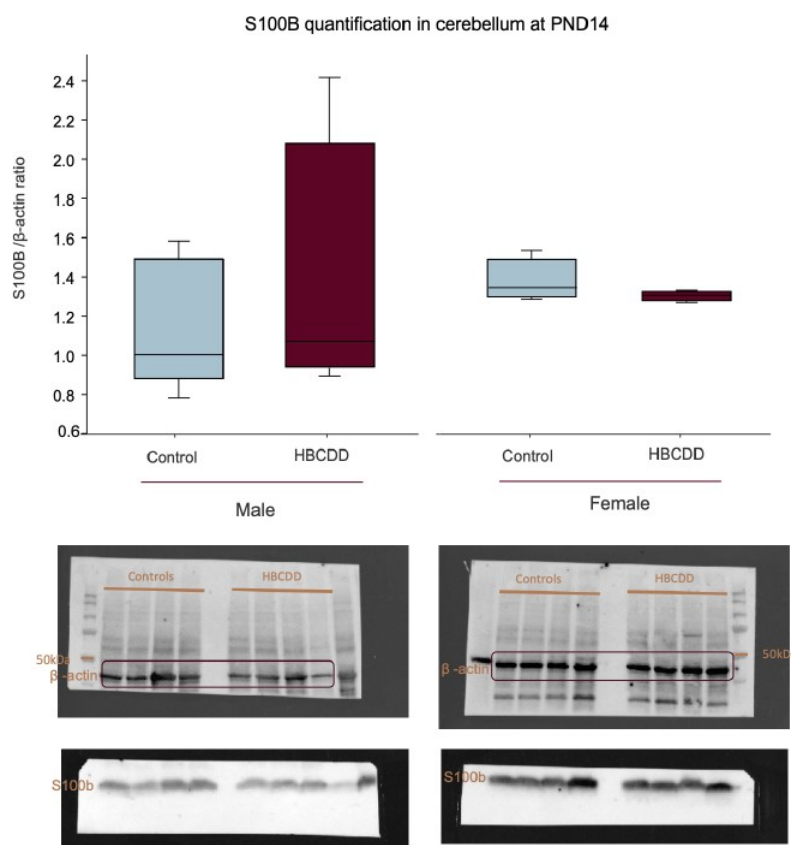


Figure 11: Effects of early α -HBCDD exposure on level of S100B in the cerebellum of PND14. As described in Material and Methods, immunoblotting was performed to assess normalized protein expression levels of S100B. For these experiments, β -actin was the loading control [76]. Results are presented as median and quartiles of the ration of S100B/ β actin. Interactions are mentioned within the text.

3.3 HBCDD-induced changes in DNA methylation

3.3.1 Identification of 6mA in HBCDD brains at PND14

In order to identify and confirm the occurrence of the new epigenetic modification of 6mA in the PND14 brains, samples of each condition were analyzed with LC-MS/MS. This reliable technique was used to prove the appearance of 6mA and to determine eventual differences in concentrations depending on the treatment.

Through LC-MS/MS, the existence and occurrence of the 6mA epigenetic modification have been proven in the 4 brain regions at PND14. Only a reduced number of samples was analyzed (2 to 3 per sex for each brain structure), as indicated on each graph. The percentage of 6mA was determined based on the ratio of unmethylated adenine and 6mA. Figure 12 displays the identification of 6mA in the frontal cortex and shows a tendency to a decrease of 6mA concentration in the HBCDD group. Remaining results for the other brain regions can be found in the supplementary information. Regarding the specificity of the result, an additional confirmation transition was applied to validate the presence of the target compounds. Confirmation of 6-methyl adenosine and adenosine presence needed a variability of around 20% for the ratio between quantification and confirmation transition [77].

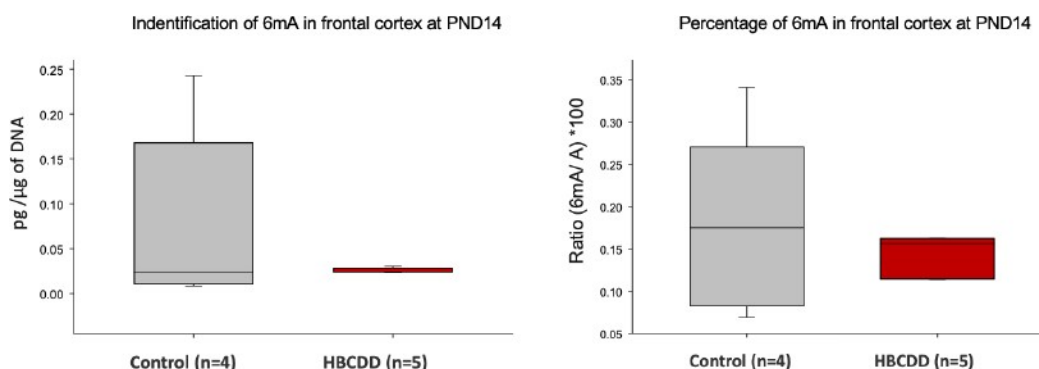


Figure 12: representative LC-MS/MS quantification of 6mA concentration (pg/μg) and percentage (ratio 6mA/A) in frontal cortex at PND14.

Taken together, these results prove for the first time the ability of α -HBCDD to impact the methylation on adenine in early life (gestation and lactation).

3.3.2 6mA validation and quantification through DotBlot

After verification of 6mA existence by LC-MS/MS, all PND14 samples were analyzed through a DotBlot technique. This technique allows detecting whether this methylation occurs in the according brain region and also whether exposure to α -HBCDD can induce dynamic changes in the levels of 6mA.

Cortex, cerebellum, brain stem and hippocampus of α -HBCDD and control groups were tested on nitrocellulose membranes and treated with 6mA specific

antibodies to state differences in 6mA levels (figure 13). Signal intensity was quantified with ImageJ.

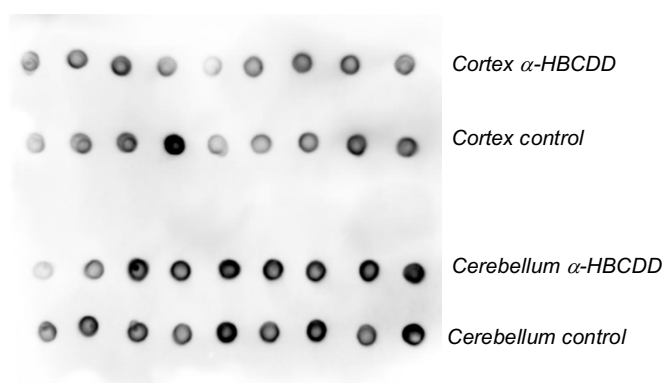
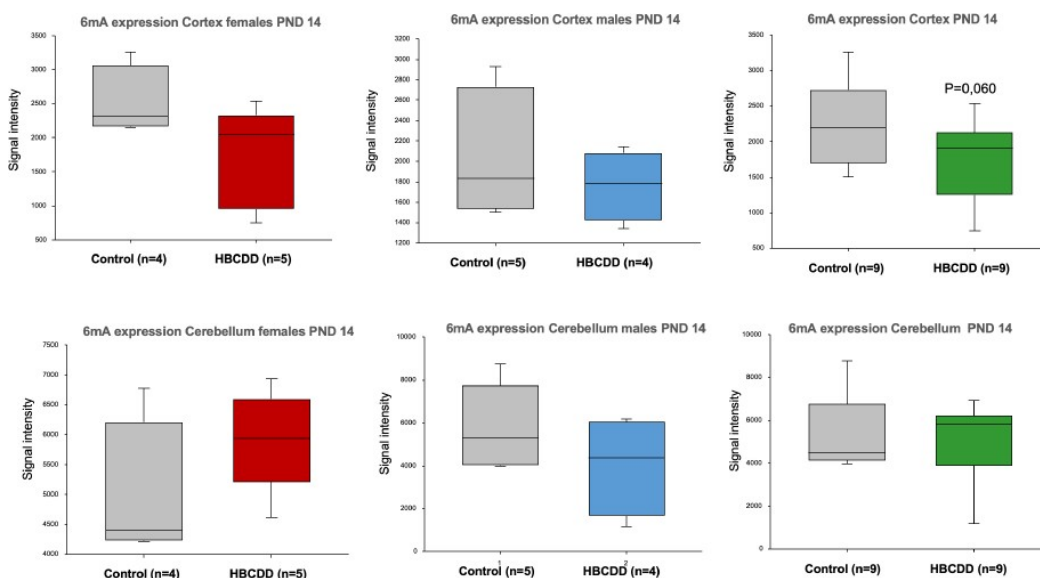


Figure 13: representative picture of a DotBlot membrane for quantification of 6mA signal intensity in cortex and cerebellum. Each dot represents one animal of the according group. All membranes were run in triplicates and on the same day. Signal was quantified with Image J and plotted with SigmaPlot Results were expressed by the mean of the 3 triplicates.

After quantification, the following results were obtained for 4 brain structures at PND14. Except for the cerebellum of the PND14 female group, there is a trend to a decrease of 6mA occurrence in the α -HBCDD groups compared to the control groups. As observed on figure 14, an effect of α -HBCDD ($p=0.06$ and $p=0.09$) has been observed in 2 regions out of the 4 investigated. As a significant litter effect has been noticed in hippocampus, the results have to be interpreted cautiously (detailed statistical analysis in supplementary information).



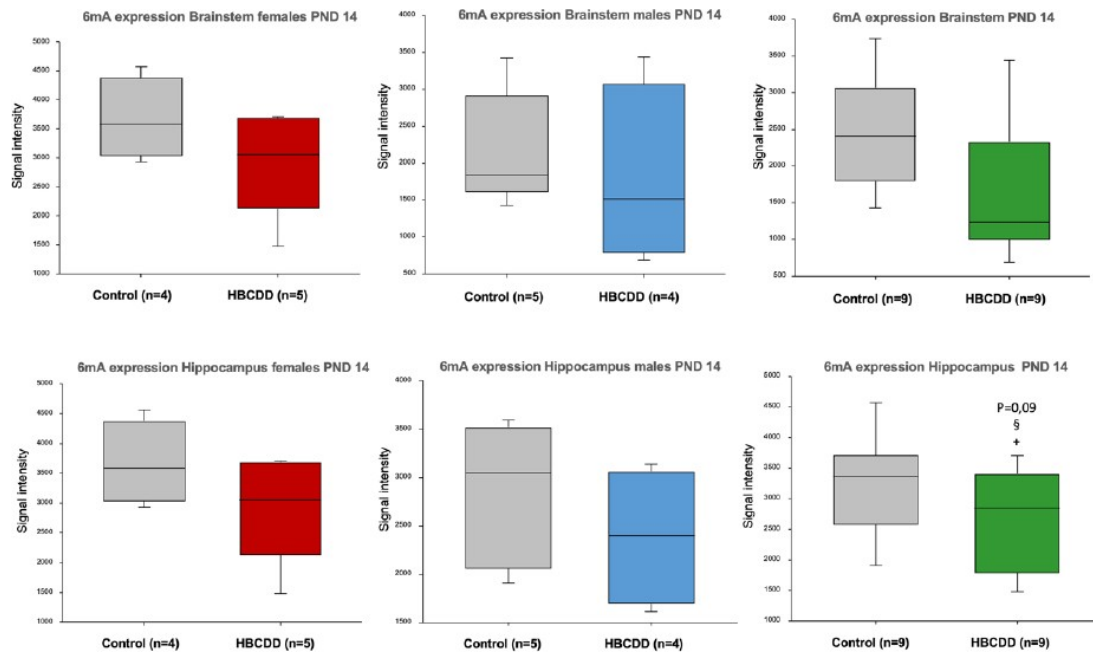


Figure 14: 6mA DotBlot quantification for cortex, cerebellum, brain stem and hippocampus of PND14 samples. Females represented in red, males in blue, total individuals in green. §= ($p<0.05$) difference significative for factor sex, += ($p<0.05$) difference significative for factor litter. $P=0,06$ and $p=0,09$, tendency for treatment effect.

Because of i) the previous behavioral data obtained at PND270 and investigation of cytochrome oxydase activity; ii) the preliminary results obtained at PND14 and iii) the constraint to precisely collect the tissue on slide, the following analysis was focused on the cerebellum. At PND270, the cerebellum was therefore analyzed as well through DotBlots, to see if the methylation profile of 6mA maintains into adult stage (figure 15). In the cerebellum, a decrease in 6mA signalintensity was stated for the α -HBCDD animals, females and males, compared to the control group. A significant interaction between HBCDD and sex was observed ($p<0.01$) (detailed statistical analysis in supplementary information). However due to significative litter effect, where pups from the same litter respond similarly to a certain stimulus, the results have to be interpreted cautiously. In that case it would not necessarily be evident that the observed differences are caused by the according treatment or by an unknown circumstance the litter was exposed to.

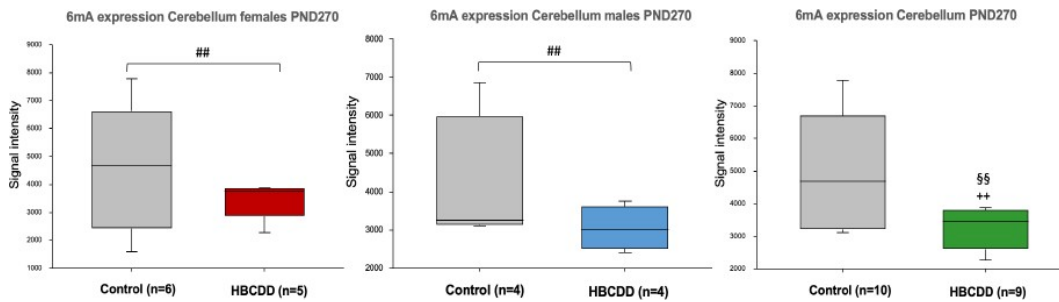


Figure 15: 6mA DotBlot quantification for PND270 cerebellum. Females represented in red, males in blue, total individuals in green. §§= ($p < 0.01$) difference significant for factor sex, ++= ($p < 0.01$) difference significant for factor litter. ## ($p < 0.01$), difference significant for the interaction sex-treatment.

3.3.3 6mA visualization through immunohistochemistry

To represent the 6mA epigenetic modification visually in the brains of PND270 animals and state possible differences, immunohistochemistry (IHC) was performed. Cells were stained with DAPI, to visualize the nucleus, and AlexaFluor 488 antibody, which bound to the primary antibody for 6mA, to tag the methylation. Full brain pictures were taken by defining tiles and multiple focus points. Following images (figure 16-19) were acquired on a Zeiss fluorescence microscope, showing for one of the first times the 6mA modification in the brain, specifically in the cerebellum. For α -HBCDD and control groups, females and males were analyzed. On figure 16, methylation can be seen to be located in the nucleus and with the intensity varying between the cells. As only two individuals/sex/group were taken to generate the present images, no quantification of the signal was done.

What was seen through IHC, was the visual validation of the 6mA modification in the cerebellar tissue. For the males, there could be a tendency to more methylation in the control and for females the other way around.

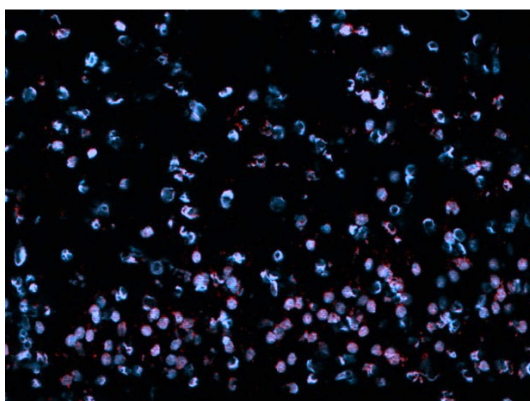


Figure 16: IHC 6mA detection in cerebellar neurons of PND270 brains, DAPI in blue, primary AB anti-6mA (1:500), secondary AB AF488 in red (1:2000), 20x objective

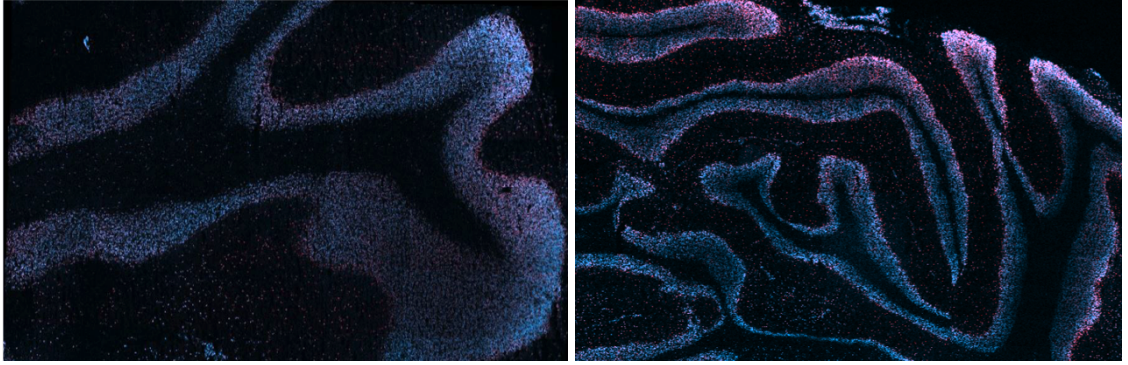


Figure 17: IHC 6mA detection in cerebellum of PND270 males, on the left α -HBCDD male, right control male. DAPI in blue, primary AB anti-6mA (1:500), secondary AB AF488 in red (1:2000), 20x objective, tiles and focus points

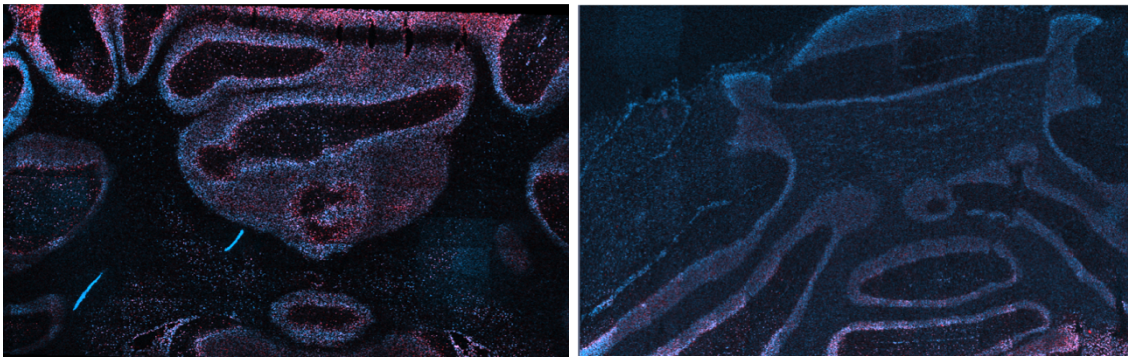


Figure 18: IHC 6mA detection in cerebellum of PND270 females, on the left α -HBCDD female, right control female. DAPI in blue, primary AB anti-6mA (1:500), secondary AB AF488 in red (1:200), 20x objective, tiles and focus points

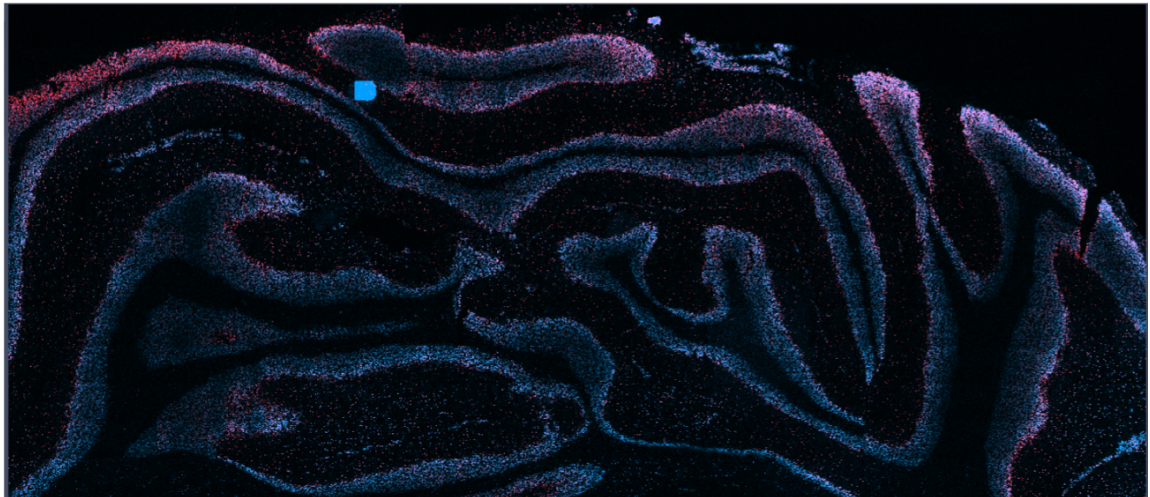


Figure 19: representative full cerebellum picture of PND270 samples, in this case male control, for 6mA detection. DAPI in blue, primary AB anti-6mA (1:500), secondary AB AF488 in red (1:2000), 20x objective, tiles and focus points

3.4 MeDIP sequencing

MeDIP-sequencing was performed on the four brain regions collected on both exposed and control pups at PND14, to evaluate changes in the complete methylation profile. Methylated DNA immunoprecipitation (MeDIP) was used to analyze specific epigenetic modifications, confirm previous results and give detailed insights in possible changes on genetic expression.

After library preparation and Illumina sequencing, data for brain stem and cerebellum of PND14 were ready for further analysis. First, data quality control (QC) was performed to i) ensure that the sequencing run had been successful, ii) that the data was of a suitable quality, and iii) that the immunoprecipitation step had enriched the samples in adenine. Initially, the number of sequences per dataset and how they aligned to the genome were extracted (table 6).

Overall, the number of reads that were mapped yielded from 44.4 and 100.5 million. Reads were aligned to the rat genome and the alignment rate was around 92- 93% with an average GC percentage of 40% and AT percentage of 60%.

Table 6: QC libraries 1-16 (PND14), general statistics on million reads that were mapped, overall alignment rate to the genome, duplication reads, average GC content and total sequences (millions). For every library, R1=forward, R2=reverse

| Sample name | M Reads Mapped | Aligned % | Dups% | GC % | M Seqs |
|------------------------|----------------|-----------|-------|------|--------|
| Lib 1 | 44.4 | 90.5% | | | |
| Lib1_S3_R1_001 | | | 8.7% | 39% | 24.5% |
| Lib1_S3_R2_001 | | | 3.1% | 41% | 24.6% |
| Lib 2 | 69.8 | 92.5% | | | |
| Lib2_S1_R1_001 | | | 11.4% | 39% | 37.7% |
| Lib2_S1_R2_001 | | | 5.8% | 41% | 37.7% |
| Lib3 | 67.0 | 92.7% | | | |
| Lib3_S3_R1_001 | | | 11.5% | 39% | 36.2% |
| Lib3_S3_R2_001 | | | 5.9% | 41% | 36.2% |
| Lib4 | 65.6% | 92.7% | | | |
| Lib4_S1_R1_001 | | | 10.4% | 39% | 35.4% |
| Lib4_S1_R2_001 | | | 5.1% | 41% | 35.4% |
| Lib5 | 69.3 | 92.3% | | | |
| Lib5_S2_R1_001 | | | 11.1% | 39% | 37.6% |
| Lib5_S2_R2_001 | | | 5.4% | 41% | 37.6% |
| Lib6 | 56.3 | 92.3% | | | |
| Lib6_S2_R1_001 | | | 11.0% | 39% | 30.5% |
| Lib6_S2_R2_001 | | | 5.4% | 41% | 30.5% |
| Lib7 | 70.4 | 92.7% | | | |
| Lib7_S3_R1_001 | | | 10.6% | 39% | 38% |
| Lib7_S3_R2_001 | | | 5.1% | 42% | 38% |
| Lib8 | 98.6 | 92.4% | | | |
| Lib8_S3_R1_001 | | | 11.8% | 39% | 53.4% |
| Lib8_S3_R2_001 | | | 5.9% | 41% | 53.4% |
| Lib10 | 75.7 | 92.5 | | | |
| Lib10_S1_R1_001 | | | 10.2% | 39% | 40.9% |
| Lib10_S1_R2_001 | | | 4.7% | 42% | 40.9% |
| Lib11 | 60.4 | 91.6% | | | |
| Lib11_S4_R1_001 | | | 9.8% | 39% | 33.0% |
| Lib11_S4_R2_001 | | | 4.4% | 42% | 33.0% |
| Lib12 | 74.3 | 92.1% | | | |
| Lib12_S4_R1_001 | | | 11.0% | 39% | 40.3% |
| Lib12_S4_R2_001 | | | 5.1% | 41% | 33.0% |
| Lib13 | 68.2 | 90.8% | | | |
| Lib13_S1_R1_001 | | | 11.4% | 39% | 37.5% |
| Lib13_S1_R2_001 | | | 5.2% | 41% | 37.5% |
| Lib14 | 57.2 | 92.0% | | | |
| Lib14_S2_R1_001 | | | 10.8% | 39% | 34.4% |
| Lib14_S2_R2_001 | | | 4.8% | 42% | 34.4% |
| Lib15 | 63.3 | 92.0% | | | |
| Lib15_S4_R1_001 | | | 10.6% | 39% | 34.4% |
| Lib15_S4_R2_001 | | | 4.8% | 42% | 34.4% |
| Lib16 | 100.5 | 91.9% | | | |
| Lib16_S2_R1_001 | | | 11.0% | 39% | 54.6% |
| Lib16_S2_R2_001 | | | 5.2% | 42% | 54.6% |
| Undetermined | 2.3 | 31.8% | | | |
| Undetermined_S0_R1_001 | | | 49.2% | 44% | 3.6 |
| Undetermined_S0_R2_001 | | | 46.3% | 45% | 3.6 |

Furthermore, the decrease in GC content can be seen in figure 20. Here the distribution of GC content per sequence generated is clearly skewed to the left, at lower % GC compared to the non-immunoprecipitated genomic DNA control (red line).

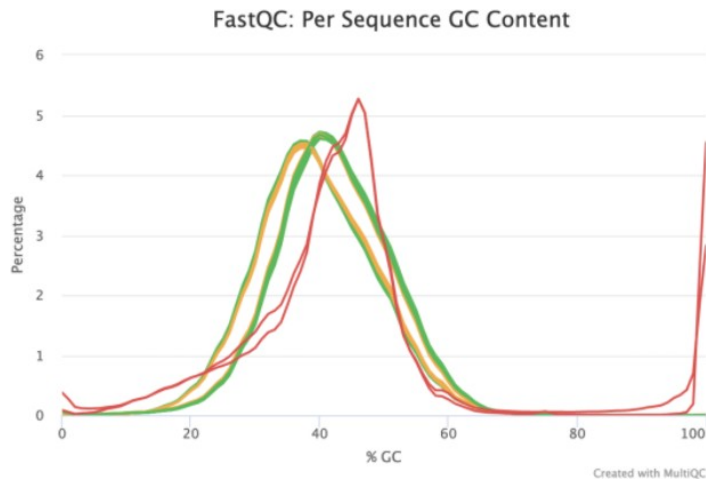


Figure 20: QC libraries 1-16 (PND14), per sequence GC content i.e average GC content of reads.

Sequencing was paired-end, covering 75 base pairs from either end of the immunoprecipitated DNA strands. Sequence quality was assessed using the Phred score, which is used to assess the quality of nucleobase identification during DNA sequencing, with FastQC, and as can be seen in figure 21. The estimated sequence quality was >30 for the full length of sequencing for all libraries, and hence of high quality.

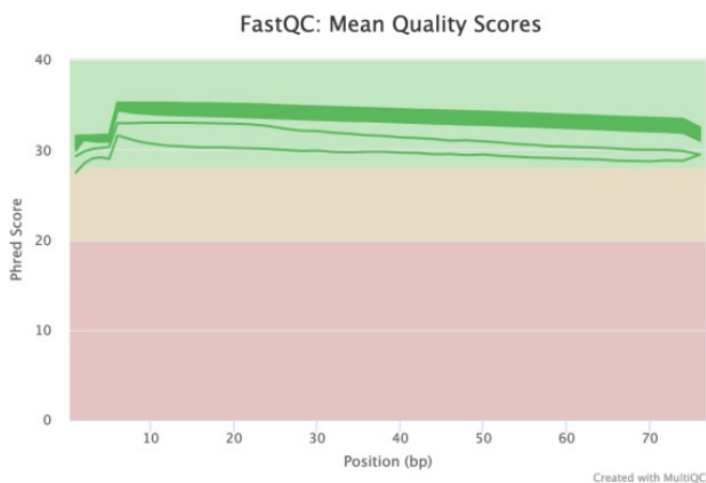
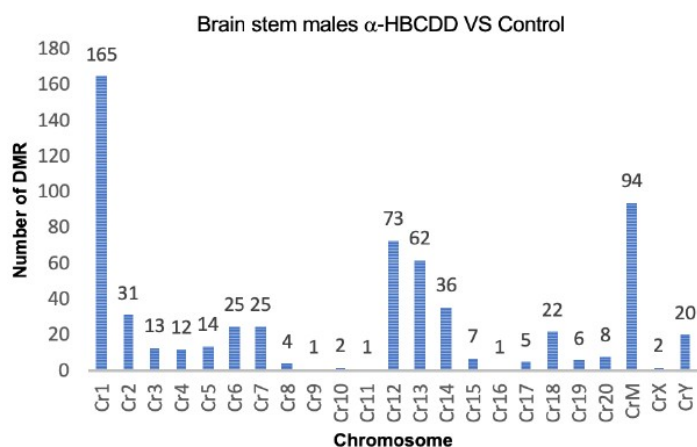
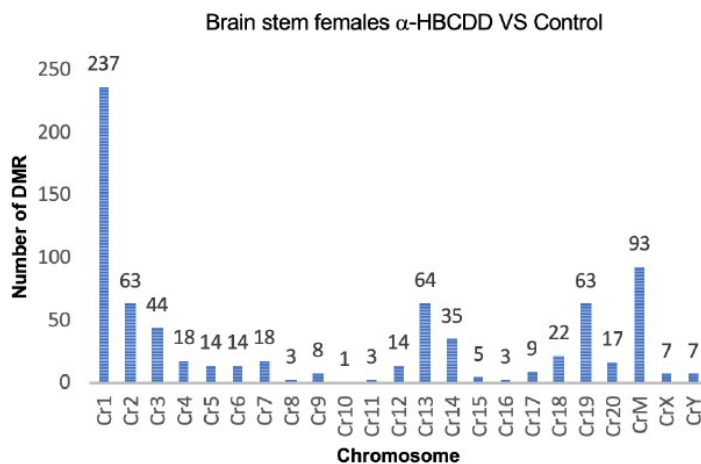


Figure 21: QC libraries 1-16 (PND14), mean quality scores. Phred scores >30 are considered high quality (green zone), 20-30 medium quality, <20 low quality.

After quality control, differential methylation was assessed using the R package MEDIPS (code in supplementary information). Aligned data was read into the R package and transformed into “Medips Sets”. During this process the genome is divided into ~5million concatenated 150bp windows, the number of sequences in each dataset aligning are counted, then normalized using the RPKM method

and normalized for adenine density to ensure that there was no bias in the statistical analysis due to certain reads having a higher percentage of adenine. Subsequently a listing of differential methylated regions, their statistical significance and log fold-change was subducted from the data for each of the brain regions studied. The following graphs (figure 22) show the number of differential methylated regions (DMR) per chromosome, for two brain regions, in females and males.

There are clear differences in the number of DMRs between the different chromosomes. Also, the total number of DMRs per brain region and sex varies. Total number in the brain stem of females is at 762 and at 629 for the males. The cerebellum of females shows 82 DMRs, the one of males 2474. This shows already that the cerebellum of the males is vulnerable to changes in methylation. The attention should also be put on changes on the Y chromosome which has a higher number of DMRs.

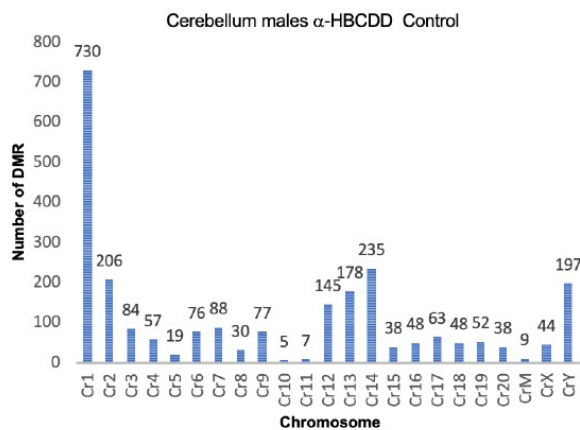
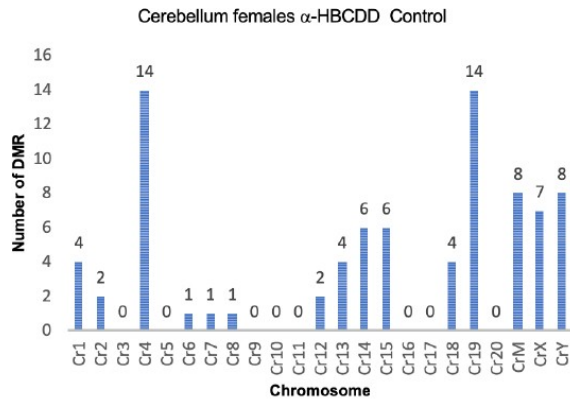


| Chromosome | lowest edgeR.logFC | highest edgeR.logFC | lowest edgeR.adj.p.value | highest edgeR.adj.p.value |
|------------|--------------------|---------------------|--------------------------|---------------------------|
| Ch1 | -3.3228 | 3.0153 | 0.0029 | 0.0217 |
| Ch2 | -1.7762 | 2.1639 | 0.0007 | 0.0330 |
| Ch3 | -4.3296 | 4.0624 | 0.0094 | 0.0483 |
| Ch4 | -3.0510 | 1.2357 | 0.0355 | 0.0032 |
| Ch5 | -4.4601 | 3.2593 | 0.0031 | 0.0017 |
| Ch6 | -1.7437 | 4.8658 | 0.0246 | 0.0397 |
| Ch7 | -2.8723 | 4.2628 | 0.0165 | 0.0094 |
| Ch8 | 0.9492 | 4.0624 | 0.0181 | 0.0483 |
| Ch9 | -3.6084 | 2.2778 | 0.0094 | 0.0140 |
| Ch10 | 3.3425 | 3.3425 | 0.0439 | 0.0439 |
| Ch11 | -1.9390 | -1.3808 | 0.0493 | 0.0217 |
| Ch12 | -1.3680 | 3.1351 | 0.0340 | 0.0321 |
| Ch13 | 0.2809 | 1.8416 | 0.0250 | 0.0020 |
| Ch14 | -1.2682 | 3.3425 | 0.0000 | 0.0439 |
| Ch15 | -1.2013 | 2.0837 | 0.0424 | 0.0092 |
| Ch16 | 1.2654 | 3.0153 | 0.0031 | 0.0217 |
| Ch17 | 0.4013 | 4.1323 | 0.0337 | 0.0282 |
| Ch18 | 0.3437 | 1.5240 | 0.0140 | 0.0379 |
| Ch19 | -0.9620 | 2.9454 | 0.0000 | 0.0023 |
| Ch20 | -4.2596 | 2.0542 | 0.0165 | 0.0025 |
| ChrM | 0.1909 | 0.9515 | 0.0001 | 0.0000 |
| ChrX | -4.1861 | 1.4368 | 0.0282 | 0.0094 |
| ChrY | -3.9740 | -1.6051 | 0.0002 | 0.0170 |

Brain stem control vs α -HBCDD females

| Chromosome | lowest edgeR.logFC | highest edgeR.logFC | lowest edgeR.adj.p.value | highest edgeR.adj.p.value |
|------------|--------------------|---------------------|--------------------------|---------------------------|
| Ch1 | -3.4607 | 0.7924 | 0.0454 | 8.12E-06 |
| Ch2 | -1.8162 | -0.4951 | 0.0069 | 0.0058 |
| Ch3 | -0.7406 | -0.3056 | 0.0221 | 0.0303 |
| Ch4 | -2.0955 | 7.5187 | 0.0338 | 0.0005 |
| Ch5 | -2.1783 | 3.0715 | 0.0336 | 0.0076 |
| Ch6 | -1.3062 | 2.4056 | 1.29E-09 | 2.38E-08 |
| Ch7 | -3.0974 | 7.2573 | 0.0360 | 0.0063 |
| Ch8 | -0.6375 | 1.5095 | 1.60E-06 | 0.0004 |
| Ch9 | -1.5868 | -1.5868 | 0.0071 | 0.0071 |
| Ch10 | -0.5769 | -0.5565 | 0.0000 | 6.18E-06 |
| Ch11 | -3.5275 | -3.5275 | 0.0272 | 0.0272 |
| Ch12 | -1.6422 | 3.2966 | 0.0434 | 0.0454 |
| Ch13 | -0.9623 | -0.2975 | 0.0321 | 0.0462 |
| Ch14 | -4.2308 | 0.9871 | 0.0289 | 3.33E-10 |
| Ch15 | -1.8897 | -1.0970 | 0.0484 | 0.0051 |
| Ch16 | -2.3494 | -2.3494 | 0.0483 | 0.0483 |
| Ch17 | -2.4957 | -0.4310 | 0.0116 | 0.0015 |
| Ch18 | -2.7054 | -0.3501 | 0.0058 | 0.0321 |
| Ch19 | -1.4691 | 0.6559 | 0.0150 | 0.0030 |
| Ch20 | -0.5552 | 0.8002 | 0.0119 | 8.17E-06 |
| ChrM | 0.2640 | 0.6867 | 0.0127 | 7.90E-09 |
| ChrX | -2.3494 | 1.5644 | 0.0483 | 0.0003 |
| ChrY | -3.3692 | -0.9157 | 0.0025 | 0.0069 |

Brain stem control vs α -HBCDD males



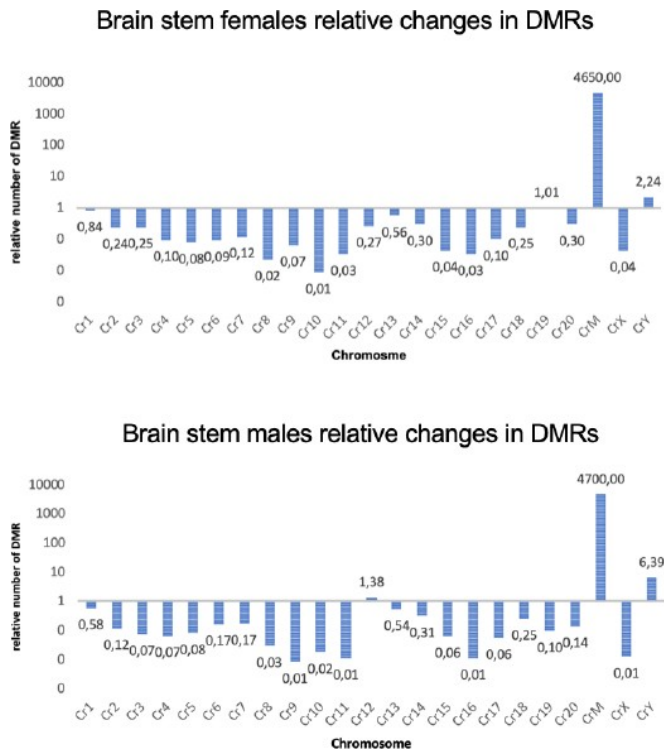
| Chromosome | lowest edgeR.logFC | highest edgeR.logFC | lowest edgeR.adj.p.value | highest edgeR.adj.p.value | Chromosome | lowest edgeR.logFC | highest edgeR.logFC | lowest edgeR.adj.p.value | highest edgeR.adj.p.value |
|------------|--------------------|---------------------|--------------------------|---------------------------|------------|--------------------|---------------------|--------------------------|---------------------------|
| Ch1 | 0,65011 | 1,52380 | 0,02781 | 0,00001 | Ch1 | -4,1415 | 4,2437 | 0,0062 | 0,0108 |
| Ch2 | -1,05452 | 0,99187 | 0,02814 | 0,01335 | Ch2 | -4,4875 | 4,2437 | 0,0002 | 0,0108 |
| Ch3 | N/A | N/A | N/A | N/A | Ch3 | -4,5379 | 3,4740 | 0,0001 | 0,0170 |
| Ch4 | -1,17306 | 0,98624 | 0,00299 | 1,91E-07 | Ch4 | -4,3248 | 4,2437 | 0,0012 | 0,0108 |
| Ch5 | N/A | N/A | N/A | N/A | Ch5 | -3,9313 | 3,4040 | 0,0308 | 0,0278 |
| Ch6 | 1,32988 | 1,32988 | 0,00059 | 0,00059 | Ch6 | -3,9313 | 2,7111 | 0,0308 | 0,0396 |
| Ch7 | -2,36431 | -2,36431 | 0,01299 | 0,01299 | Ch7 | -3,9313 | 2,7697 | 0,0308 | 0,0257 |
| Ch8 | -2,33119 | -2,33119 | 0,00397 | 0,00397 | Ch8 | -4,1415 | 3,3305 | 0,0062 | 0,0441 |
| Ch9 | N/A | N/A | N/A | N/A | Ch9 | -3,5134 | 3,3305 | 0,0021 | 0,0441 |
| Ch10 | N/A | N/A | N/A | N/A | Ch10 | -3,1529 | 2,5133 | 0,0441 | 0,0163 |
| Ch11 | N/A | N/A | N/A | N/A | Ch11 | -2,9013 | 3,4040 | 0,0135 | 0,0278 |
| Ch12 | -0,44981 | -0,43384 | 0,00023 | 0,00015 | Ch12 | -4,1415 | -0,4913 | 0,0062 | 0,0351 |
| Ch13 | -4,20623 | 0,47690 | 0,03574 | 0,04527 | Ch13 | -4,0048 | 3,4040 | 0,0185 | 0,0278 |
| Ch14 | -0,85590 | -0,42081 | 0,00001 | 0,04645 | Ch14 | -4,2663 | 1,7407 | 0,0020 | 0,0330 |
| Ch15 | -1,47559 | -1,03916 | 0,00104 | 0,04878 | Ch15 | -4,1415 | 2,2565 | 0,0062 | 0,0423 |
| Ch16 | N/A | N/A | N/A | N/A | Ch16 | -2,3918 | 2,4570 | 0,0434 | 0,0257 |
| Ch17 | N/A | N/A | N/A | N/A | Ch17 | -3,3444 | 3,3305 | 0,0102 | 0,0441 |
| Ch18 | -0,70777 | -0,46883 | 0,00309 | 0,00894 | Ch18 | -4,0048 | 1,0727 | 0,0185 | 0,0397 |
| Ch19 | 0,55468 | 3,29254 | 0,03416 | 0,02385 | Ch19 | -3,2196 | 2,3984 | 0,0278 | 0,0396 |
| Ch20 | N/A | N/A | N/A | N/A | Ch20 | -2,4999 | -0,5257 | 0,0396 | 0,0465 |
| ChrM | 0,30515 | 0,59778 | 0,01826 | 0,00001 | ChrM | -1,2302 | -0,3640 | 1,29E-08 | 0,0364 |
| ChrX | -7,19325 | -1,16552 | 0,04210 | 0,02642 | ChrX | -4,6337 | 1,5946 | 3,42E-05 | 0,0315 |
| ChrY | -7,19325 | -0,78042 | 0,04210 | 0,00219 | ChrY | -1,9590 | -0,9451 | 0,0116 | 0,0001 |

Cerebellum control vs α -HBCDD females

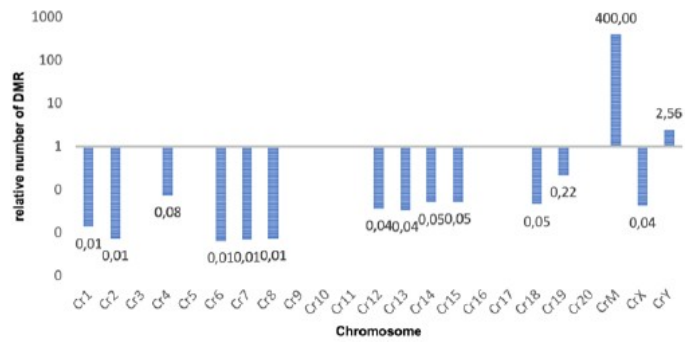
Cerebellum control vs α -HBCDD males

Figure 22: Total number of differential methylated regions per chromosome for brain stem (top) and cerebellum (bottom) of PND14 females and males. Summary tables of lowest and highest logFC and adj. p values for every chromosome.

As the chromosomes all differ in length, this can also be taken into consideration to evaluate the relative difference in DMRs. The following graphs (figure 23) show this relation. As the mitochondrial chromosome is very small in size, it gets clear, that important differences can be seen at this level. The relative number of changes in DMRs ranges at around 4700 for the mitochondrial chromosomes but rarely reaches a higher number than 0.5 for the remaining chromosomes.



Cerebellum females relative changes in DMRs



Cerebellum males relative changes in DMRs

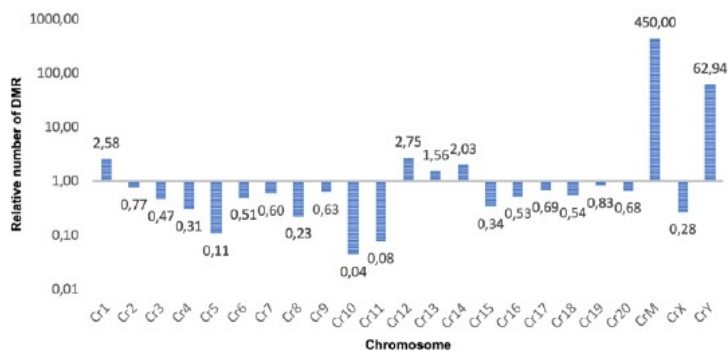


Figure 23: relative number of DMRs on a log scale, according to the different sizes of the chromosomes. Brain stem and cerebellum, females and males.

4. Discussion

Over the last decades, neurodegenerative diseases have become more and more frequent [2]. Multiple recent studies confirm that early life exposure to persistent organic pollutants may affect the susceptibility for disease development in later life. Even though, details about the etiology of many diseases are still missing, such perturbations during sensitive developmental phases might play a key role [2]. Recent work of our lab shows that epidemiological studies associate environmentally persistent organic pollutant exposure to neurodegenerative diseases including Alzheimer's and Parkinson's diseases [2]. Polybrominated diphenyl ethers (PBDE), polybromo biphenyls (PBB) as well as brominated flame retardants (BFRs) have been linked to ADHD and ASD [2].

Due to their psycho-chemical properties, BFRs widely occur in the environment and enter the food chain via fish, eggs, milk and meat products [78]. Food products, polluted indoor atmospheres, and dust are therefore the major sources of human BFR exposure. A recent study conducted by Maurice and colleagues pointed out that HBCDD, administered at doses consistent with realistic human exposure levels, induces neurobehavioral disorders in rats emerging during the first 4 weeks of postnatal life and persisting in adulthood[1]. These include anxiety, locomotion and sexual activity disorders [1, 79]. Similar findings were stated for adult rats at PND 270. In addition to this, the activity of CO was evaluated on PND270 brains and diminutions were found in the auditory, visual, motor, limbic systems as well as in hypothalamus and brain stem [62]. On the basis of this preliminary data, assessing the developmental neurotoxicity of BFRs appears as a major concern. Such results suggest that HBCDD could be a developmental neurotoxicant and raise the question of its ability to facilitate the occurrence of neurodegenerative phenotypes in the offspring.

Building on these previous results, the current study aimed to identify the epigenetic and immune response of the brain tissues which were exposed to the pollutant throughout gestation and lactation. As the focus of the research group is on early life adversities, which can come in various forms, this exposure to an environmental pollutant during a total of 42 days (~ 3 years in humans [3]) constitutes a good example of an early life stressor. As the quantity of α -HBCDD

administration was calculated according to the available human exposure data; it is an accurate representation to assess potential human toxicity. Environmental stressors experienced *in utero* or early postnatal life have been established in the literature to be associated with later-life neurological disorders [21, 22]. Importantly, as the maturing brain goes through some critical windows, environmental stressors can have an important impact which can persist over time. When talking about environmental stressors, epigenetics, as being the link between environment, genes and phenotypes, have to be in focus. This study investigated 6mA as a new epigenetic mark and wanted to identify dynamic changes as a response to α -HBCDD exposure. Multiple techniques, including LC-MS/MS and DotBlots, were used to confirm the occurrence of this new methylation and state differences in concentration of 6mA. Neuroinflammation levels have been assessed because previous studies showed already that POPs can be transferred from mother to foetus through the placenta [43] and if this is the case they might influence the developing organism, including the brain.

This work demonstrates, for the first time, that α -HBCDD, a pollutant of global concern, if absorbed by the mother, can be transferred to the pups, pass the blood-brain barrier and subsequently modifies cerebral DNA methylation profiles as well as increases levels of neuroinflammation level.

It was important at the start of this study to establish that HBCDD could be detected in the offspring brain. Using LC-MS/MS, we were able to confirm that HBCDD could be detected in the brain of pups that were exposed to HBCDD during gestation and sacrificed at PND1, confirming that HBCDD can be incorporated by living organisms and therefore also enrich in the food chain. This means that from an early stage on, HBCDD, where α and γ isomers appear to be the most represented ones, can be integrated in neuronal structures and could affect the brain development and the functioning of different brain structures.

After demonstrating that the pollutant was able to enter the brain, neuroinflammation levels were assessed.

Indeed, there is now significant evidence that immune dysfunction and neuroinflammation are highly involved in the emergence of neurodegenerative diseases, both leading to a chronic state of low-grade inflammation in the central nervous

system [80]. Activation of microglia by POPs and their ability to alter the permeability of the blood brain barrier could play a key role in these processes [81]. Western blots were used to assess the level of S100B, a neuroinflammatory marker, in PND14 samples. This marker can be found predominantly in astroglia cells of the CNS and an increase in its expression level can be linked to neuro-pathological disorders, like AD or DS, where it can lead to neurodegeneration [75]. S100B was significantly increased in the cortex of α -HBCDD exposed males and females whereas in the cerebellum no significant difference was detected. This proves, that if pollutants, in this case α -HBCDD, enter the brain during critical developmental stages, they will trigger an increased immune activity, including the production of inflammatory mediators like cytokines, who then promote neuroinflammation [38]. This reaction might lead to the damage or even degeneration of neurons, altering the functioning and development of the brain. Neuroinflammation was unequivocally observed at PND14 and the question remains as to whether it persists at adult age. Analyses are currently being performed on the 3 other regions of the brain at PND14 and PND270 as well as GFAP measurements to possibly confirm the ability of α -HBCDD to induce brain immune response.

For the epigenetic analyses, we initially confirmed that 6mA is a new genuine epigenetic mark on eukaryotic DNA in addition to its well-established role in eukaryotic RNA. We started with the confirmation through LC-MS/MS. 6mA concentration and percentage, which was the ratio of 6mA and A, were determined for cortex, cerebellum, hippocampus and brain stem of PND14 samples. Using this technique, the results confirmed the presence of 6mA in brain tissue and prove the ability of HBCDD to impact the methylation on adenine in early life (gestation and lactation). Building up on this confirmation, cortex, cerebellum, brain stem and hippocampus of PND14 samples were tested for differences in 6mA signal intensity with an independent technique, namely DotBlots. Although we did not see a statistically significant differences in 6mA levels, but overall there appeared to be a trend to reduced 6mA levels after α -HBCDD exposure. An exception to this was the case of the cerebellum of the α -HBCDD exposed females. Chronic stress can implicate an increase in 6mA in the PFC in mice [33], whereas a decrease in 6mA was linked to augmented tumorigenesis [31]. As there are obviously variable findings, further investigation on this topic is required.

The hippocampus showed a significant litter effect, which describes the tendency of individuals of the same litter to respond in a similar way to a stimulus [82], so the results have to be interpreted cautiously. As the DotBlot technique brings along many variables and a rather fluctuating reproducibility, it should be confirmed by means of other techniques. Nevertheless, as these experiments were always run in triplicates, a clear tendency of 6mA intensity can be subducted and used for further considerations.

Due to previous results on the PND270 samples, including CO activity measurement and behavioral testing, and to the fact that these samples were already prepared as 20 μm thick histological slices, we decided to focus on the cerebellum for the purpose of writing this report. To allow as much precision as possible and ensure that only cerebellar DNA was extracted from the samples, the cerebellum was chosen as the first brain structure of interest. The cortex will be the next step in the 6mA screening for the PND270 samples. Again, there was a clear tendency for a decrease in 6mA intensity. The LC-MS/MS analysis currently under performance on all the animals and should confirm this result. As we observed both a litter effect and a significant interaction between treatment and sex, these results have to be interpreted cautiously.

PND270 brain slices were used for immunohistochemistry assays, to demonstrate visually the appearance of the 6mA modification in brain tissue. As the optimization of the protocol was not trivial, only a reduced number of representative samples were used. We were able to visually demonstrate for first time this methylation in neuronal tissue and we were able to detect it abundantly in the nucleus of the cells. By acquiring full brain, in this case full cerebellum, pictures, differences in the methylation profiles could be seen. To improve this technique markers like MAP2, which visualizes neuronal dendrites, or NeuN, identifying only neurons, should be added [83]. Subsequently, only neurons could be analyzed and cell subsets could be distinguished. It would also be profitable to use a confocal microscope to enhance the quality of the pictures. Once the whole protocol is set, fluorescent pictures should be quantified and concrete differences in methylation obtained. At this point of the project, the technique was used to add visual proof of the identification of 6mA to other techniques.

Finally, we immunoprecipitated and sequenced DNA from the PND14 samples. For this report, results of cerebellum and brain stem were available, while cortex

and hippocampus results are still being processed. By using the MeDIP protocol and subsequent Illumina sequencing, the goal was to confirm the occurrence of 6mA and identify specific differences between α -HBCDD and control groups. Quality control confirmed the successful sequencing and enrichment in adenine through prior immunoprecipitation. By using the R package MeDIPS, a listing of differential methylated regions per chromosome was collected. As described in the results, there is a considerable variability in the number of DMRs between the different chromosomes. As regards the brain stem, chromosome 1, for example, might play a more important role, since it shows a higher number of DMRs than the other chromosomes. Also, the total number of DMRs varies between brain regions and sex. In comparison to approximately 700 DMRs in the brain stem, the cerebellum of males shows about 2500. Changes in the Y chromosome should also be noticed. Since previous results showed that HBCDD can act as an endocrine disruptor [1, 62], this would require further investigation. As the chromosomes differ in size, the relative number of DMRs shows that, by reason of its small size (0.02 Mb), the mitochondrial DNA is highly affected by methylation changes.

On the basis of this data, the next step that needs to be performed is the annotation of the DMR to the neighboring genes. Once this has been done, we can determine how changes in methylation affect gene expression and if changes in 6mA levels suppress or induce gene expression. Afterwards, functions of the associated genes can be assessed and a possible link to later impairments can be drawn.

As a prospect to this project, we could focus on the completion of the sequencing analysis of all the samples of PND14 and PN270, and then later possibly on the detailed investigation of the gene expression. Furthermore, more brain structures should be tested for their neuroinflammation level, by using more markers; and specific vulnerable brain regions where α -HBCDD has an influence. This appears necessary to assess the magnitude of impairments caused by early life exposure to pollutants. Also, the usage of the RNA, which has been left out of this, should be envisaged. Similar studies showed that, prenatal exposure to specific air pollution results in a reduced neurogenesis in the hippocampus and increased neuroinflammation, paired with behavioral impairments like depressive or disturbed

food-seeking behavior [84]. Therefore, the specific mode of action of different pollutants needs to be clarified. Overall, the preliminary data generated in this report are highly promising, opening up a new field of investigation in the host research group. Our proof that α -HBCDD can enter the brain in very early developmental stages and provoke significant neuroinflammation is a first hint as to the potential toxicity of this compound. The further identification and observation of dynamic changes of the 6mA epigenetic mark, opens the door to deeper epigenetic analysis and demonstrates the impact of environmental stressors.

5. Conclusion

This study demonstrated for the first time, that a specific persistent organic pollutant, namely α -HBCDD, can be transferred from mother to pups and pass the brain-blood barrier at a very early stage in life, and therefore is classified as an environmental early life stressor. Once incorporated in the brain, this pollutant will trigger neuroinflammation which later on could interfere with brain development and functioning. Furthermore, 6mA has been identified as genuine epigenetic mark through different techniques. As a response to α -HBCDD treatment during gestation and lactation, dynamic changes and a tendency to a decrease in 6mA occurrence in the brain have been noticed. Corresponding Illumina® sequencing proved, that many differential methylated regions can be identified on the different chromosomes. From this, detailed gene analysis is required and the impact of early life pollutant exposure on gene expression could reveal possible links to disease phenotypes or impairments later in life. To set these results into connection with the behavioral phenotypes of the initial study, according brain regions would need to be analyzed in detail and molecular mechanism which underly these impairments would need to be revealed. Here, a first look on how/where in the brain α -HBCDD can act has been proposed and further investigation could define the toxicity of this pollutant.

6. References

1. Maurice, N., et al., *Short-term effects of a perinatal exposure to the HBCDD α -isomer in rats: Assessment of early motor and sensory development, spontaneous locomotor activity and anxiety in pups*. Neurotoxicology and Teratology, 2015. **52**: p. 170-180.
2. Grova, N., et al., *Epigenetic and Neurological Impairments Associated with Early Life Exposure to Persistent Organic Pollutants*. International Journal of Genomics, 2019. **2019**: p. 19.
3. Sengupta, P., *The Laboratory Rat: Relating Its Age With Human's*. International journal of preventive medicine, 2013. **4**(6): p. 624-630.
4. Barker, D.J.C.O., *Infant mortality, childhood nutrition, and ischaemic heart disease in England and Wales*. Lancet, 1986. **1**(8489): p. 1077-1081.
5. Anda, R., et al., *Adverse Childhood Experiences and Frequent Headaches in Adults*. Headache: The Journal of Head and Face Pain, 2010. **50**(9): p. 1473-1481.
6. Friedman, E.M., et al., *Early life adversity and adult biological risk profiles*. Psychosomatic medicine, 2015. **77**(2): p. 176-185.
7. Korkeila, J., et al., *Childhood adversities as predictors of incident coronary heart disease and cerebrovascular disease*. Heart, 2010. **96**(4): p. 298-303.
8. Eriksson, M., K. Räikkönen, and J.G. Eriksson, *Early life stress and later health outcomes—findings from the Helsinki Birth Cohort Study*. American Journal of Human Biology, 2014. **26**(2): p. 111-116.
9. Scott, K.M., et al., *Childhood Adversity, Early-Onset Depressive/Anxiety Disorders, and Adult-Onset Asthma*. Psychosomatic Medicine, 2008. **70**(9): p. 1035-1043.
10. Brown, D.W., et al., *Adverse childhood experiences are associated with the risk of lung cancer: a prospective cohort study*. BMC Public Health, 2010. **10**(1): p. 20.
11. Dube, S.R., et al., *Cumulative Childhood Stress and Autoimmune Diseases in Adults*. Psychosomatic Medicine, 2009. **71**(2): p. 243-250.
12. Ehler, U., *Enduring psychobiological effects of childhood adversity*. Psychoneuroendocrinology, 2013. **38**(9): p. 1850-1857.
13. Kessler, R.C., et al., *Childhood adversities and adult psychopathology in the WHO World Mental Health Surveys*. British Journal of Psychiatry, 2010. **197**(5): p. 378-385.
14. Spitzer, C., et al., *Gender-specific association between childhood trauma and rheumatoid arthritis: A case-control study*. Journal of Psychosomatic Research, 2013. **74**(4): p. 296-300.
15. Miller, G.E., et al., *Divergent transcriptional profiles in pediatric asthma patients of low and high socioeconomic status*. Pediatric Pulmonology, 2018. **53**(6): p. 710-719.
16. Turner, J.D., *Holistic, personalized, immunology? The effects of socioeconomic status on the transcriptional milieu of immune cells*. Pediatric Pulmonology, 2018. **53**(6): p. 696-697.
17. Daskalakis, N.P., et al., *The three-hit concept of vulnerability and resilience: Toward understanding adaptation to early-life adversity outcome*. Psychoneuroendocrinology, 2013. **38**(9): p. 1858-1873.
18. Li, X., et al., *"Three Hits" Hypothesis for Developmental Origins of Health and Diseases in View of Cardiovascular Abnormalities*. Birth Defects Research, 2017. **109**(10): p. 744-757.
19. Elwenspoek, M.M.C., et al., *The effects of early life adversity on the immune system*. Psychoneuroendocrinology, 2017. **82**: p. 140-154.
20. Lenroot, R.K. and J.N. Giedd, *Brain development in children and adolescents:*

- Insights from anatomical magnetic resonance imaging*. Neuroscience & Biobehavioral Reviews, 2006. **30**(6): p. 718-729.
21. Landrigan Philip, J., et al., *Early Environmental Origins of Neurodegenerative Disease in Later Life*. Environmental Health Perspectives, 2005. **113**(9): p. 1230-1233.
 22. Tran, N.Q.V. and K. Miyake, *Neurodevelopmental Disorders and Environmental Toxicants: Epigenetics as an Underlying Mechanism*. International Journal of Genomics, 2017. **2017**: p. 23.
 23. Miller, D.B. and J.P. O'Callaghan, *Do early-life insults contribute to the late-life development of Parkinson and Alzheimer diseases?* Metabolism - Clinical and Experimental, 2008. **57**: p. S44-S49.
 24. Borenstein, A.R., C.I. Copenhagen, and J.A. Mortimer, *Early-Life Risk Factors for Alzheimer Disease*. Alzheimer Disease & Associated Disorders, 2006. **20**(1): p. 63-72.
 25. Foster, H.D., *Why the preeminent risk factor in sporadic Alzheimer's disease cannot be genetic*. Medical Hypotheses, 2002. **59**(1): p. 57-61.
 26. Leenen, F.A.D., C.P. Muller, and J.D. Turner, *DNA methylation: conducting the orchestra from exposure to phenotype?* Clinical Epigenetics, 2016. **8**(1): p. 92.
 27. Mazzio, E.A. and K.F.A. Soliman, *Basic concepts of epigenetics*. Epigenetics, 2012. **7**(2): p. 119-130.
 28. Levenson, V.V., *DNA methylation as a universal biomarker*. Expert Review of Molecular Diagnostics, 2010. **10**(4): p. 481-488.
 29. Luo, G.-Z., et al., *DNA N6-methyladenine: a new epigenetic mark in eukaryotes?* Nature Reviews Molecular Cell Biology, 2015. **16**: p. 705.
 30. Wu, T.P., et al., *DNA methylation on N6-adenine in mammalian embryonic stem cells*. Nature, 2016. **532**: p. 329.
 31. Xiao, C.-L., et al., *N⁶-Methyladenine DNA Modification in the Human Genome*. Molecular Cell, 2018. **71**(2): p. 306-318.e7.
 32. Xie, Q., et al., *N⁶-methyladenine DNA Modification in Glioblastoma*. Cell, 2018. **175**(5): p. 1228-1243.e20.
 33. Yao, B., et al., *DNA N6-methyladenine is dynamically regulated in the mouse brain following environmental stress*. Nature Communications, 2017. **8**(1): p. 1122.
 34. Bazan, N.G., et al., *Chapter 34 - Neuroinflammation*, in *Basic Neurochemistry (Eighth Edition)*, S.T. Brady, et al., Editors. 2012, Academic Press: New York. p. 610-620.
 35. Chen, W.-W., X. Zhang, and W.-J. Huang, *Role of neuroinflammation in neurodegenerative diseases (Review)*. Molecular medicine reports, 2016. **13**(4): p. 3391-3396.
 36. DiSabato, D.J., N. Quan, and J.P. Godbout, *Neuroinflammation: the devil is in the details*. Journal of Neurochemistry, 2016. **139**(S2): p. 136-153.
 37. Milatovic, D., et al., *Chapter 55 - Neuroinflammation and Oxidative Injury in Developmental Neurotoxicity*, in *Reproductive and Developmental Toxicology (Second Edition)*, R.C. Gupta, Editor. 2017, Academic Press. p. 1051-1061.
 38. Brockmeyer, S. and A. D'Angiulli, *How air pollution alters brain development: the role of neuroinflammation*. Translational neuroscience, 2016. **7**(1): p. 24-30.
 39. Calderón-Garcidueñas, L., et al., *Air Pollution and Children: Neural and Tight Junction Antibodies and Combustion Metals, the Role of Barrier Breakdown and Brain Immunity in Neurodegeneration*. Journal of Alzheimer's disease : JAD, 2014. **43**.
 40. Levesque, S., et al., *Diesel Exhaust Activates and Primes Microglia: Air Pollution, Neuroinflammation, and Regulation of Dopaminergic Neurotoxicity*. Environmental Health Perspectives, 2011. **119**(8): p. 1149-1155.
 41. Levesque, S., et al., *The role of MAC1 in diesel exhaust particle-induced microglial activation and loss of dopaminergic neuron function*. Journal of

- Neurochemistry, 2013. **125**(5): p. 756-765.
42. Ransohoff, R.M., *How neuroinflammation contributes to neurodegeneration*. Science, 2016. **353**(6301): p. 777-783.
 43. Zhang, X., et al., *Transplacental transfer of polycyclic aromatic hydrocarbons in paired samples of maternal serum, umbilical cord serum, and placenta in Shanghai, China*. Environmental Pollution, 2017. **222**: p. 267-275.
 44. Liu, J., et al., *Bisphenol A Metabolites and Bisphenol S in Paired Maternal and Cord Serum*. Environmental Science & Technology, 2017. **51**(4): p. 2456-2463.
 45. Chin-Chan, M., J. Navarro-Yepes, and B. Quintanilla-Vega, *Environmental pollutants as risk factors for neurodegenerative disorders: Alzheimer and Parkinson diseases*. Frontiers in Cellular Neuroscience, 2015. **9**(124).
 46. Organization, W.H. *Persistent organic pollutants (POPs)*. 2019 [cited 2019 21.09.2019]; Available from: https://www.who.int/foodsafety/areas_work/chemical-risks/pops/en/.
 47. La Merrill, M., et al., *Toxicological Function of Adipose Tissue: Focus on Persistent Organic Pollutants*. Environmental Health Perspectives, 2013. **121**(2): p. 162-169.
 48. Hendriks, H.S. and R.H.S. Westerink, *Neurotoxicity and risk assessment of brominated and alternative flame retardants*. Neurotoxicology and Teratology, 2015. **52**: p. 248-269.
 49. Medecine, U.S.N.L.o. *1,2,5,6,9,10-Hexabromocyclododecane*. 2019 [cited 2019 21.09.2019]; Available from: <https://pubchem.ncbi.nlm.nih.gov/compound/18529>.
 50. Miller-Rhodes, P., et al., *Prenatal exposure to the brominated flame retardant hexabromocyclododecane (HBCD) impairs measures of sustained attention and increases age-related morbidity in the Long-Evans rat*. Neurotoxicology and Teratology, 2014. **45**: p. 34-43.
 51. Fromme, H., et al., *Polybrominated diphenyl ethers (PBDEs), hexabromocyclododecane (HBCD) and "novel" brominated flame retardants in house dust in Germany*. Environment International, 2014. **64**: p. 61-68.
 52. Harrad, S. and M.A.-E. Abdallah, *Concentrations of Polybrominated Diphenyl Ethers, Hexabromocyclododecanes and Tetrabromobisphenol-A in Breast Milk from United Kingdom Women Do Not Decrease over Twelve Months of Lactation*. Environmental Science & Technology, 2015. **49**(23): p. 13899-13903.
 53. Aylward, L.L. and S.M. Hays, *Biomonitoring-based risk assessment for hexabromocyclododecane (HBCD)*. International Journal of Hygiene and Environmental Health, 2011. **214**(3): p. 179-187.
 54. Abdallah, M.A.-E., S. Harrad, and A. Covaci, *Hexabromocyclododecanes and Tetrabromobisphenol-A in Indoor Air and Dust in Birmingham, UK: Implications for Human Exposure*. Environmental Science & Technology, 2008. **42**(18): p. 6855-6861.
 55. Abdallah, M.A.-E., et al., *Hexabromocyclododecanes In Indoor Dust From Canada, the United Kingdom, and the United States*. Environmental Science & Technology, 2008. **42**(2): p. 459-464.
 56. UNEP, *Report of the Persistent Organic Pollutants Review Committee on the work of its seventh meeting*. 2011. p. 30.
 57. Genskow, K.R., et al., *Selective damage to dopaminergic transporters following exposure to the brominated flame retardant, HBCDD*. Neurotoxicology and teratology, 2015. **52**(Pt B): p. 162-169.
 58. Ibhazehiebo, K., et al., *1,2,5,6,9,10- α -Hexabromocyclododecane (HBCD) Impairs Thyroid Hormone-Induced Dendrite Arborization of Purkinje Cells and Suppresses Thyroid Hormone Receptor-Mediated Transcription*. The Cerebellum, 2011. **10**(1): p. 22-31.
 59. Refatto, V., et al., *Parallel in vivo and in vitro transcriptomics analysis reveals calcium and zinc signalling in the brain as sensitive targets of HBCD*

- neurotoxicity. Archives of Toxicology, 2018. **92**(3): p. 1189-1203.
60. Heeb, N.V., et al., *Regio- and stereoselective isomerization of hexabromocyclododecanes (HBCDs): Kinetics and mechanism of γ - to α -HBCD isomerization*. Chemosphere, 2008. **73**(8): p. 1201-1210.
 61. Jondreville, C., et al., *Hens can ingest extruded polystyrene in rearing buildings and lay eggs contaminated with hexabromocyclododecane*. Chemosphere, 2017. **186**: p. 62-67.
 62. Zalka, L., *Etude de la neurotoxicité de l' α -Hexabromocyclododecane lors d'une exposition gestationnelle et lactationnelle sur le rat wistar*. 2015, Université de Lorraine. p. 42.
 63. Semple, B.D., et al., *Brain development in rodents and humans: Identifying benchmarks of maturation and vulnerability to injury across species*. Progress in Neurobiology, 2013. **106-107**: p. 1-16.
 64. Wong-Riley, M.T.T., *Cytochrome oxidase: an endogenous metabolic marker for neuronal activity*. Trends in Neurosciences, 1989. **12**(3): p. 94-101.
 65. Ploteau, S., et al., *Distribution of persistent organic pollutants in serum, omental, and parietal adipose tissue of French women with deep infiltrating endometriosis and circulating versus stored ratio as new marker of exposure*. Environment International, 2016. **97**: p. 125-136.
 66. Antignac, J.P., et al., *Country-specific chemical signatures of persistent organic pollutants (POPs) in breast milk of French, Danish and Finnish women*. Environmental Pollution, 2016. **218**: p. 728-738.
 67. Ploteau, S., et al., *Associations between internal exposure levels of persistent organic pollutants in adipose tissue and deep infiltrating endometriosis with or without concurrent ovarian endometrioma*. Environment International, 2017. **108**: p. 195-203.
 68. Sathe, K., et al., *S100B is increased in Parkinson's disease and ablation protects against MPTP-induced toxicity through the RAGE and TNF- α pathway*. Brain, 2012. **135**(11): p. 3336-3347.
 69. Candela, P., et al., *In vitro discrimination of the role of LRP1 at the BBB cellular level: Focus on brain capillary endothelial cells and brain pericytes*. Brain Research, 2015. **1594**: p. 15-26.
 70. Emerce, E., et al., *Carbon Nanotube- and Asbestos-Induced DNA and RNA Methylation Changes in Bronchial Epithelial Cells*. Chemical Research in Toxicology, 2019. **32**(5): p. 850-860.
 71. De Nys, S., et al., *Temporal variability of global DNA methylation and hydroxymethylation in buccal cells of healthy adults: Association with air pollution*. Environment International, 2018. **111**: p. 301-308.
 72. Hardy, E.M., et al., *Multi-residue analysis of organic pollutants in hair and urine for matrices comparison*. Forensic Science International, 2015. **249**: p. 6-19.
 73. Bharagava, R.N., et al., *Chapter 26 Applications of Metagenomics in Microbial Bioremediation of Pollutants From Genomics to Environmental Cleanup, in Microbial Diversity in the Genomic Era*. 2019. p. 459-477.
 74. Illumina. *An introduction to Next-Generation Sequencing Technology*. 2017 [cited 2019 21.09.2019]; Available from: www.illumina.com/technology/next-generation-sequencing.html.
 75. Shapiro, L.A., L.A. Bialowas-McGoey, and P.M. Whitaker-Azmitia, *Effects of S100B on Serotonergic Plasticity and Neuroinflammation in the Hippocampus in Down Syndrome and Alzheimer's Disease: Studies in an S100B Overexpressing Mouse Model*. Cardiovascular psychiatry and neurology, 2010. **2010**: p. 153657.
 76. Kuntz, M., et al., *Bexarotene Promotes Cholesterol Efflux and Restricts Apical-to-Basolateral Transport of Amyloid- β Peptides in an In Vitro Model of the Human Blood-Brain Barrier*. Journal of Alzheimer's disease : JAD, 2015. **48**.
 77. Grova, N., G. Salqu  bre, and B. Appenzeller, *Gas chromatography-tandem*

- mass spectrometry analysis of 52 monohydroxylated metabolites of polycyclic aromatic hydrocarbons in hairs of rats after controlled exposure*. Analytical and bioanalytical chemistry, 2013. **405**.
78. Chain, E.P.o.C.i.t.F., *Scientific Opinion on Hexabromocyclododecanes (HBCDDs) in Food*. EFSA Journal, 2011. **9**(7): p. 2296.
 79. Olivier, B., et al., *Perinatal exposure of rat pups to the HexaBromoCycloDoDecane (HBCDD) α -isomer affects sexual maturation and copulatory behavior at the adult stage*. Vol. 259. 2016. S111.
 80. Dipasquale, V., et al., *Neuroinflammation in Autism Spectrum Disorders: Role of High Mobility Group Box 1 Protein*. International journal of molecular and cellular medicine, 2017. **6**(3): p. 148-155.
 81. Block, M.L. and L. Calderón-Garcidueñas, *Air pollution: mechanisms of neuroinflammation and CNS disease*. Trends in Neurosciences, 2009. **32**(9): p. 506-516.
 82. *Litter Effect*, in *Wiley StatsRef: Statistics Reference Online*.
 83. Tanapat, P. *Neuronal Cell Markers*. 2013 2019-08-18 [cited 2019 21.09.2019]; Available from: <https://www.labome.com/method/Neuronal-Cell-Markers.html>.
 84. Woodward, N.C., et al., *Prenatal and early life exposure to air pollution induced hippocampal vascular leakage and impaired neurogenesis in association with behavioral deficits*. Translational Psychiatry, 2018. **8**(1): p. 261.

Picture references

Figure 2:

J. Michael Sanders, Gabriel A. Knudsen, Linda S. Birnbaum, The Fate of β -Hexabromocyclododecane in Female C57BL/6 Mice, *Toxicological Sciences*, Volume 134, Issue 2, August 2013, Pages 251–257,
<https://academic.oup.com/toxsci/article-abstract/134/2/251/1633071?redirectedFrom=fulltext>

Figure 5:

Instruction Manual

Accel-NGS® 1S Plus DNA Library Kit for Illumina® Platforms

http://www.tataa.com/wp-content/uploads/2012/10/Accel-NGS%C2%AE-1S-Plus-DNA-Library-Kit-for-Illumina%C2%AE-Platforms_Manual.pdf

Figure 6:

SPRIselect user guide

https://research.fhcrc.org/content/dam/stripe/hahn/methods/mol_biol/SPRIselect%20User%20Guide.pdf




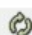






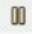
Figure 7:

An introduction to next-generation sequencing technology








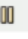

https://www.illumina.com/documents/products/illumina_sequencing_introduction.pdf

7. Supplementary information

• KingFisher Plate 1 Protocol

| Tip1 | KingFisher tip comb | | |
|--|---------------------------|------------------------|--|
|  CollectBeads1 | Step 1 | (A) - Beads only | |
| | Collect count | 5 | |
| | Collect time [s] | 30 | |
|  Block sol 1 - wash 1 | Step 1 | (B) - Block solution 1 | |
| Beginning of step | Precollect | No | |
| | Release beads | Yes | |
| Mixing / pause: | Mixing time, speed | 00:05:00, Slow | |
| | Pause for manual handling | No | |
| End of step | Postmix | No | |
| | Collect count | 3 | |
| | Collect time [s] | 10 | |
|  Block sol 1 - wash 2 | Step 1 | (C) - Block solution 1 | |
| Beginning of step | Precollect | No | |
| | Release beads | Yes | |
| Mixing / pause: | Mixing time, speed | 00:05:00, Slow | |
| | Pause for manual handling | No | |
| End of step | Postmix | No | |
| | Collect count | 3 | |
| | Collect time [s] | 10 | |
|  Ab-beads complex | Step 1 | (D) - Ab-beads complex | |
| Beginning of step | Precollect | No | |
| | Release beads | Yes | |
| Mixing / pause: | Mixing time, speed | 06:00:00, Slow | |
| | Pause for manual handling | No | |
| End of step | Postmix | No | |
| | Collect count | 3 | |
| | Collect time [s] | 10 | |
|  Block sol 2 - wash 1 | Step 1 | (E) - Block solution 2 | |
| Beginning of step | Precollect | No | |
| | Release beads | Yes | |
| Mixing / pause: | Mixing time, speed | 00:03:00, Slow | |
| | Pause for manual handling | No | |
| End of step | Postmix | No | |
| | Collect count | 3 | |
| | Collect time [s] | 10 | |
|  Block sol 2 - wash 2 | Step 1 | (F) - Block solution 2 | |
| Beginning of step | Precollect | No | |
| | Release beads | Yes | |
| Mixing / pause: | Mixing time, speed | 00:03:00, Slow | |
| | Pause for manual handling | No | |
| End of step | Postmix | No | |
| | Collect count | 3 | |
| | Collect time [s] | 10 | |
|  Block sol 2 - wash 3 | Step 1 | (G) - Block solution 2 | |
| Beginning of step | Precollect | No | |
| | Release beads | Yes | |
| Mixing / pause: | Mixing time, speed | 00:03:00, Slow | |
| | Pause for manual handling | No | |
| End of step | Postmix | No | |
| | Collect count | 3 | |
| | Collect time [s] | 10 | |
|  Block sol 3 | Step 1 | (H) - Block solution 3 | |
| Beginning of step | Precollect | No | |
| | Release beads | Yes | |
| Mixing / pause: | Mixing time, speed | 00:30:00, Slow | |
| | Pause for manual handling | No | |
| End of step | Postmix | No | |
| | Collect beads | No | |
|  Pause2 | Step 1 | (H) - Block solution 3 | |
| | Message | Be ready for plate 2 | |
|  CollectBeads2 | Step 1 | (H) - Block solution 3 | |
| | Collect count | 3 | |
| | Collect time [s] | 15 | |
|  Pause1 | Step 1 | (H) - Block solution 3 | |
| | Message | Add plate 2 | |

• KingFisher Plate 2 Protocol

| Tip2 | KingFisher tip comb | | |
|---|------------------------------|---------------------------|---------------------------|
|  | Immunoprecipitation | Step 2 | (A) - Immunoprecipitation |
| | Beginning of step | Precollect | No |
| | | Release beads | Yes |
| | Mixing / pause: | Mixing time, speed | 16:00:00, Slow |
| | | Pause for manual handling | No |
| | End of step | Postmix | No |
| | | Collect count | 3 |
| | | Collect time [s] | 10 |
|  | IP buffer - wash 1 | Step 2 | (B) - IP wash 1 |
| | Beginning of step | Precollect | No |
| | | Release beads | Yes |
| | Mixing / pause: | Mixing time, speed | 00:03:00, Slow |
| | | Pause for manual handling | No |
| | End of step | Postmix | No |
| | | Collect count | 3 |
| | | Collect time [s] | 10 |
|  | IP buffer - wash 2 | Step 2 | (C) - IP wash 2 |
| | Beginning of step | Precollect | No |
| | | Release beads | Yes |
| | Mixing / pause: | Mixing time, speed | 00:03:00, Slow |
| | | Pause for manual handling | No |
| | End of step | Postmix | No |
| | | Collect count | 3 |
| | | Collect time [s] | 10 |
|  | IP stringent buffer - wash 1 | Step 2 | (D) - IP stringent wash 1 |
| | Beginning of step | Precollect | No |
| | | Release beads | Yes |
| | Mixing / pause: | Mixing time, speed | 00:03:00, Slow |
| | | Pause for manual handling | No |
| | End of step | Postmix | No |
| | | Collect count | 3 |
| | | Collect time [s] | 10 |
|  | IP stringent buffer - wash 2 | Step 2 | (E) - IP stringent wash 2 |
| | Beginning of step | Precollect | No |
| | | Release beads | Yes |
| | Mixing / pause: | Mixing time, speed | 00:03:00, Slow |
| | | Pause for manual handling | No |
| | End of step | Postmix | No |
| | | Collect beads | No |
|  | Pause1 | Step 2 | (E) - IP stringent wash 2 |
| | | Message | Be ready for elution |
|  | CollectBeads1 | Step 2 | (E) - IP stringent wash 2 |
| | | Collect count | 3 |
| | | Collect time [s] | 10 |
|  | Pause2 | Step 2 | (E) - IP stringent wash 2 |
| | | Message | Add plate 3 |
|  | Elution | Step 2 | (F) - Elution |
| | Beginning of step | Precollect | No |
| | | Release beads | Yes |
| | Mixing / pause: | Mixing time, speed | 00:00:10, Medium |
| | | Pause for manual handling | No |
| | End of step | Postmix | No |
| | | Collect beads | No |

- Library preparation protocol

Prepare the Library

For best results, please follow these suggestions:

- To maximize efficient use of enzyme reagents, remove enzyme tubes from -20 °C storage and place on ice, NOT in a cryocooler, for at least 10 minutes to allow reagents to reach 4 °C prior to pipetting.
- Attempting to pipette enzymes at -20 °C may result in a shortage of enzyme reagents.**
- After thawing reagents, vortex (except enzymes) to mix well.
- For heavily damaged samples, it is important to use a quality control metric to analyze DNA integrity and purity. If you have questions related to sample quality, please contact Technical Support.
- If preparing multiple libraries at once, assemble reagent master mixes for **Adaptase**, **Extension**, **Ligation**, and **Indexing PCR** steps and scale volumes as appropriate, using 5% excess volume to compensate for pipetting loss.
- Always add enzymes last to master mixes, immediately before adding to samples. Gently vortex to mix.
- Before starting, prepare a fresh 80% ethanol solution. Approximately 5 ml will be used per sample.

DNA Fragmentation:

- Determine DNA concentration and purity. Concentration may be assessed using a NanoDrop with A260/280 ratio or another absorbance-based method or, if samples are dsDNA, by using Qubit or another fluorimetric-based method. Accurate determination of DNA input amount is important for determining the number of PCR cycles required at the end of the protocol.
- Fragment the DNA. Multiple fragmentation methods are available; this kit was validated on and provides size selection guidelines for DNA fragmented by Covaris to 200 bp or 350 bp. Do not denature double-stranded samples prior to fragmentation. When possible, fragment dsDNA because the yield of molecules with the desired insert size will be more consistent. Fragmentation of ssDNA may result in shorter fragments and lower library yield. Please note that ssDNA cannot be visualized by Bioanalyzer.

Optional Concentration Step:

If you have performed enzymatic reactions, including enzymatic fragmentation, or your fragmented DNA concentration is too low to provide sufficient quantity in the 15 µl DNA starting volume specified in the Adaptase step, concentrate with a Zymo DNA Clean & Concentrator kit or other method and elute in 15 µl of Low EDTA TE buffer.

Otherwise, skip to the Denaturation Step.

Denaturation:

- Due to the short incubation time of the Denaturation step, pre-assemble the Adaptase Reaction Mix, except for Enzymes G4, G5, and G6, and place on ice.
- Pre-heat the thermocycler to 95 °C until all samples are ready to be loaded.

Incubation Conditions

95 °C for 2 minutes, lid heating ON
Immediately place on ice for 2 minutes then
proceed to Adaptase Step

- Add 15 µl of fragmented DNA to a 0.2 ml PCR tube.
- Place each sample in the thermocycler and incubate for 2 minutes to denature the DNA. Upon completion, place tube in ice **immediately** for 2 minutes. Proceed directly to the Adaptase step to preserve the maximum amount of ssDNA substrate.

Adaptase:

- Load the Adaptase Thermocycler Program on the thermocycler and pause it at the first step to pre-heat to 37 °C until all samples are loaded.

Adaptase Thermocycler Program

37 °C for 15 minutes, lid heating ON
95 °C for 2 minutes, lid heating ON
4 °C hold

- On ice, make the Adaptase Reaction Mix with the following amounts of each reagent.

| Assembly Order | Reagent | Volume per Reaction |
|---------------------|-------------|---------------------|
| Pre-assemble | Low EDTA TE | 11.5 µl |
| | Buffer G1 | 4 µl |
| | Reagent G2 | 4 µl |
| | Reagent G3 | 2.5 µl |
| Add just before use | Enzyme G4 | 1 µl |
| | Enzyme G5 | 1 µl |
| | Enzyme G6 | 1 µl |

- Add 25 µl of the Adaptase Reaction Mix to each PCR tube containing a 15 µl denatured DNA sample. The final reaction volume for each sample is 40 µl. Gently vortex to mix the reaction well and spin down. Place in the thermocycler and run the program.

Extension:

- Load the Extension Thermocycler Program on the thermocycler and pause it at the first step (98 °C) until all samples are loaded.

Extension Thermocycler Program

98 °C for 30 seconds, lid heating ON
63 °C for 15 seconds, lid heating ON
68 °C for 5 minutes, lid heating ON
4 °C hold

- On ice, make an Extension Reaction Mix with the following amounts of each reagent.

| Assembly Order | Reagent | Volume per Reaction |
|---------------------|-------------|---------------------|
| Pre-assemble | Low EDTA TE | 18.5 µl |
| | Reagent Y1 | 2 µl |
| | Reagent W2 | 7 µl |
| | Buffer W3 | 17.5 µl |
| Add just before use | Enzyme W4 | 2 µl |

- Add 47 µl to each PCR tube containing a 40 µl Adaptase Reaction. The final reaction volume is 87 µl. Gently vortex to mix the reaction well and spin down. Place in the thermocycler and run the program.

Post-Extension SPRI:

For inputs ≥ 1 ng, clean up the Extension Reaction using SPRIselect beads (refer to Appendix) and freshly prepared 80% ethanol:

| Input | Sample | SPRI | Elution |
|---------------------|------------|--------------------------|------------|
| ≥ 1 ng, 200 bp | 87 μ l | 104 μ l (ratio: 1.2) | 20 μ l |
| ≥ 1 ng, 350 bp | | 70 μ l (ratio: 0.8) | |

For inputs < 1 ng, clean up the Extension Reaction with two consecutive clean-ups using SPRIselect beads (refer to Appendix) and freshly prepared 80% ethanol:

| Input | Sample | SPRI | Elution |
|------------------|----------------------|--|--------------------------|
| < 1 ng, 200 bp | 1 st SPRI | 87 μ l | 104 μ l (ratio: 1.2) |
| | 2 nd SPRI | 50 μ l (1 st SPRI eluate) | 60 μ l (ratio: 1.2) |
| < 1 ng, 350 bp | 1 st SPRI | 87 μ l | 70 μ l (ratio: 0.8) |
| | 2 nd SPRI | 50 μ l (1 st SPRI eluate) | 40 μ l (ratio: 0.8) |



Store eluate at 4 °C until ready to proceed.

Ligation:

- Load the Ligation Thermocycler Program on the thermocycler and pause it at the first step (25 °C) until all samples are mixed and loaded.

Ligation Thermocycler Program

25 °C for 15 minutes, lid heating ON
4 °C hold

- On ice, make a Ligation Reaction Mix with the following amounts of each reagent.

| Assembly Order | Reagent | Volume per Reaction |
|---------------------|-------------|---------------------|
| Pre-assemble | Low EDTA TE | 4 μ l |
| | Buffer B1 | 4 μ l |
| | Reagent B2 | 10 μ l |
| Add just before use | Enzyme B3 | 2 μ l |

- Add 20 μ l of the Ligation Reaction Mix to each PCR tube containing a 20 μ l SPRI Step eluate. The final reaction volume is 40 μ l. Gently vortex to mix the reaction well and spin down. Place in the thermocycler and run the program.

Post-Ligation SPRI:

Clean up the Ligation Reaction using SPRIselect beads (refer to Appendix) and freshly prepared 80% ethanol:

| Input | Sample | SPRI | Elution |
|--------|------------|-------------------------|------------|
| 200 bp | 40 μ l | 40 μ l (ratio: 1.0) | 20 μ l |
| 350 bp | | 32 μ l (ratio: 0.8) | |



Store eluate at 4 °C until ready to proceed.

Indexing PCR:

- Add indexing reagent(s) directly to sample.

| Reagent | Volume Added to Each Sample (Using SI-IL1SP-12A) | Volume Added to Each Sample (Using DI-IL1SP-48) |
|---------------------------|--|---|
| Reagent R1 (index primer) | 5 μ l | - |
| Index D50X | - | 2.5 μ l |
| Index D7XX | - | 2.5 μ l |

- On ice, make a PCR Reaction Mix with the following amounts of each reagent.

| Assembly Order | Reagent | Volume per Reaction |
|---------------------|-------------|---------------------|
| Pre-assemble | Low EDTA TE | 10 μ l |
| | Reagent W2 | 4 μ l |
| | Buffer W3 | 10 μ l |
| Add just before use | Enzyme W4 | 1 μ l |

- Mix well, and then add 25 μ l of the PCR Reaction Mix to the library + indexing primer mix (25 μ l). Mix by pipetting. The final reaction volume is 50 μ l.
- Perform each PCR reaction in a thermocycler with the following conditions:

Indexing PCR Thermocycler Program

98 °C for 30 seconds, lid heating ON
PCR Cycles:
98 °C for 10 seconds, lid heating ON
60 °C for 30 seconds, lid heating ON
68 °C for 60 seconds, lid heating ON
Hold at 4 °C

| Input Quantity | Recommended PCR Cycles* |
|----------------|-------------------------|
| 1 μ g | 3 |
| 100 ng | 4 |
| 10 ng | 7 |
| 1 ng | 10 |
| 100 pg | 14 |
| 10 pg | 17 |

* The number of cycles required to produce enough library for sequencing will depend on input quantity and quality. In the case of low quality samples, the number of cycles required may vary based on the quality of the sample and amount of adaptable DNA present. Approximate guidelines for high quality DNA are shown in the table above, but the exact number of cycles required must be determined by the user.

Post-PCR SPRI:

Clean up the PCR Reaction using SPRIselect beads (for protocol, see Appendix) and freshly prepared 80% ethanol:

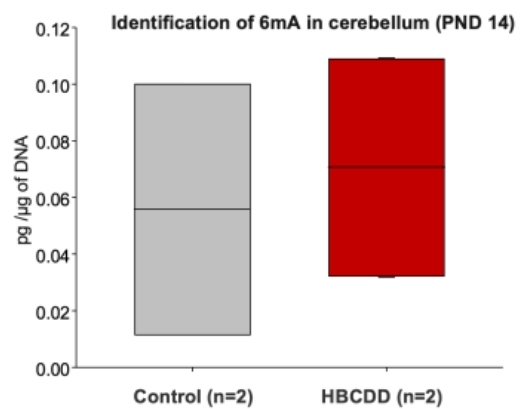
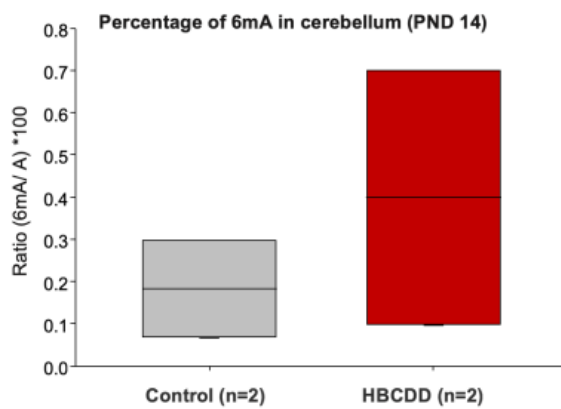
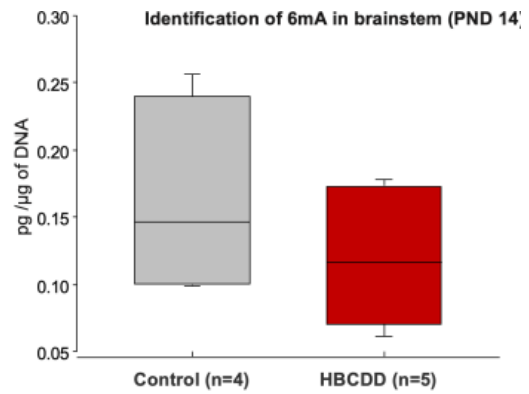
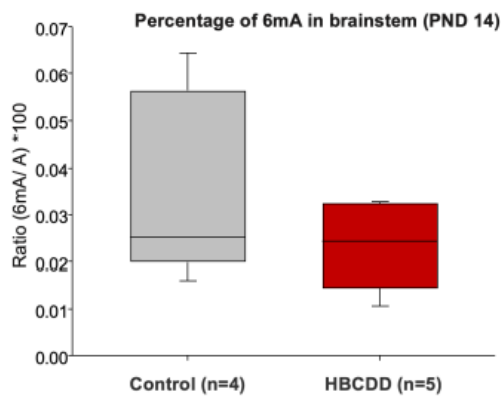
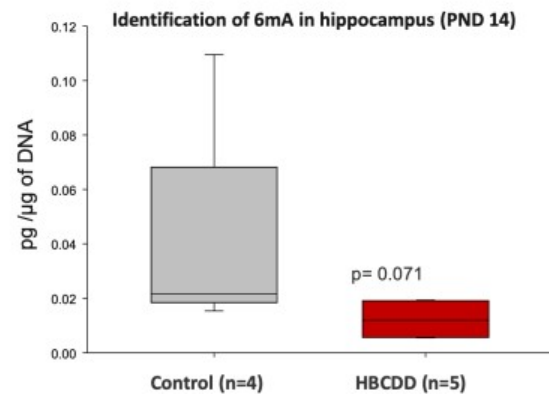
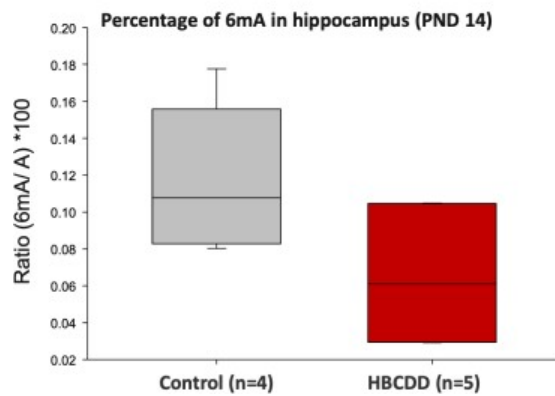
| Input | Sample | SPRI | Elution |
|--------|------------|----------------------------|------------|
| 200 bp | 50 μ l | 42.5 μ l (ratio: 0.85) | 20 μ l |
| 350 bp | | | |



Store freshly prepared libraries at 4°C.

The library is now ready for quantification and sequencing.

- LC-MS/MS quantification for hippocampus, brain stem and cerebellum



- **Statistical analysis for Dotblot results at PND14**

| | | | | | |
|--|-----------|---------------|----------------|----------------|------------------|
| Response for Cortex at PND14 | | | | | |
| | Df | Sum Sq | Mean Sq | F value | Pr(>F) |
| Treatment * | 1 | 1266441 | 1266441 | 4,4739 | 0,06051 |
| Sex § | 1 | 177570 | 177570 | 0,6273 | 0,44673 |
| Litter + | 4 | 2328464 | 582116 | 2,0564 | 0,16194 |
| Treatment:Sex ⌘ | 1 | 6987 | 6987 | 0,0247 | 0,87829 |
| Residuals | 10 | 2830739 | 283074 | | |
| Response for Cerebellum at PND14 | | | | | |
| | Df | Sum Sq | Mean Sq | F value | Pr(>F) |
| Treatment * | 1 | 486724 | 486724 | 0,1771 | 0,6828 |
| Sex § | 1 | 1229907 | 1229907 | 0,4476 | 0,5186 |
| Litter + | 4 | 1,4E+07 | 3510226 | 1,2775 | 0,3417 |
| Treatment:Sex ⌘ | 1 | 5943833 | 5943833 | 2,1631 | 0,1721 |
| Residuals | 10 | 2,7E+07 | 2747801 | | |
| Response for Brainstem at PND14 | | | | | |
| | Df | Sum Sq | Mean Sq | F value | Pr(>F) |
| Treatment * | 1 | 2699399 | 2699399 | 2,646 | 0,1349 |
| Sex § | 1 | 58819 | 58819 | 0,0577 | 0,8151 |
| Litter + | 4 | 455903 | 113976 | 0,1117 | 0,9755 |
| Treatment:Sex ⌘ | 1 | 782598 | 782598 | 0,7671 | 0,4017 |
| Residuals | 10 | 1E+07 | 1020185 | | |
| Response for hippocampus at PND14 | | | | | |
| | Df | Sum Sq | Mean Sq | F value | Pr(>F) |
| Treatment * | 1 | 1197009 | 1197009 | 3,3148 | 0,09867 |
| Sex § | 1 | 2113571 | 2113571 | 5,853 | 0,03611 |
| Litter + | 4 | 4998480 | 1249620 | 3,4605 | 0,05066 |
| Treatment:Sex ⌘ | 1 | 2585 | 2585 | 0,0072 | 0,93424 |
| Residuals | 10 | 3611098 | 361110 | | |
| Response for Cerebellum at PND270 | | | | | |
| | Df | Sum Sq | Mean Sq | F value | Pr(>F) |
| Treatment * | 1 | 1479124 | 1479124 | 2,894 | 0,1327 |
| Sex § | 1 | 8050192 | 8050192 | 15,751 | 0,0054 |
| Litter + | 8 | 4,1E+07 | 5159639 | 10,095 | 0,00317 |
| Treatment:Sex ⌘ | 1 | 7779534 | 7779534 | 15,221 | 0,00589 |
| Residuals | 7 | 3577685 | 511098 | | |

- **R code used to analyze the Illumina sequencing Data for PND14 samples**

```
library(BSgenome.Rnorvegicus.UCSC.rn6)
library(MEDIPS)
setwd("/mnt/pcpnfs/homedirs/dii6/6mA_HBCDD/bam/UCSC")
dir.create("/mnt/pcpnfs/homedirs/dii6/6mA_HBCDD/medips_sets")

lib_2_MeDIP=MEDIPS.createSet(file="Lib2.bam",
BSgenome="BSgenome.Rnorvegicus.UCSC.rn6", uniq=1, extend=300, shift=0, paired = TRUE,
window_size=150)
lib_3_MeDIP=MEDIPS.createSet(file="Lib3.bam",
BSgenome="BSgenome.Rnorvegicus.UCSC.rn6", uniq=1, extend=300, shift=0, paired = TRUE,
window_size=150)
lib_6_MeDIP=MEDIPS.createSet(file="Lib6.bam",
BSgenome="BSgenome.Rnorvegicus.UCSC.rn6", uniq=1, extend=300, shift=0, paired = TRUE,
window_size=150)
lib_7_MeDIP=MEDIPS.createSet(file="Lib7.bam",
BSgenome="BSgenome.Rnorvegicus.UCSC.rn6", uniq=1, extend=300, shift=0, paired = TRUE,
window_size=150)
lib_10_MeDIP=MEDIPS.createSet(file="Lib10.bam",
BSgenome="BSgenome.Rnorvegicus.UCSC.rn6", uniq=1, extend=300, shift=0, paired = TRUE,
window_size=150)
lib_11_MeDIP=MEDIPS.createSet(file="Lib11.bam",
BSgenome="BSgenome.Rnorvegicus.UCSC.rn6", uniq=1, extend=300, shift=0, paired = TRUE,
window_size=150)
lib_14_MeDIP=MEDIPS.createSet(file="Lib14.bam",
BSgenome="BSgenome.Rnorvegicus.UCSC.rn6", uniq=1, extend=300, shift=0, paired = TRUE,
window_size=150)
lib_15_MeDIP=MEDIPS.createSet(file="Lib15.bam",
BSgenome="BSgenome.Rnorvegicus.UCSC.rn6", uniq=1, extend=300, shift=0, paired = TRUE,
window_size=150)

setwd("/mnt/pcpnfs/homedirs/dii6/6mA_HBCDD/medips_sets")

save(lib_2_MeDIP, file="Lib2_set")
save(lib_3_MeDIP, file="Lib3_set")
save(lib_6_MeDIP, file="Lib6_set")
save(lib_7_MeDIP, file="Lib7_set")
save(lib_10_MeDIP, file="Lib10_set")
save(lib_11_MeDIP, file="Lib11_set")
save(lib_14_MeDIP, file="Lib14_set")
save(lib_15_MeDIP, file="Lib15_set")

# load("Lib2_set")
# load("Lib3_set")
# load("Lib6_set")
# load("Lib7_set")
# load("Lib10_set")
# load("Lib11_set")
# load("Lib14_set")
# load("Lib15_set")

#####
### Normalisation AND calibration plots
#####
setwd("/mnt/pcpnfs/homedirs/dii6/6mA_HBCDD/medips_sets")

CS = MEDIPS.couplingVector(pattern="A", refObj=lib_6_MeDIP)

save(CS, file = "150WS_2gps_Calibration_set_lib_6_CS-A")
# load("150WS_2gps_Calibration_set_lib_6_CS-A")

#####
### Methylation profiling & genomewide coverage
#####

dir.create("/mnt/pcpnfs/homedirs/dii6/6mA_HBCDD/CS-A")
dir.create("/mnt/pcpnfs/homedirs/dii6/6mA_HBCDD/CS-A/medips_MvF_files")
setwd("/mnt/pcpnfs/homedirs/dii6/6mA_HBCDD/CS-A/medips_MvF_files")
```

```

# Female cerebellum C vs HBCDD
MP_FC_cereb = MEDIPS.meth(MSet1=lib_6_MeDIP, CSet=CS,p.adj="BH",
diff.method="edgeR",
                        MeDIP=T, CNV=F, minRowSum=20)
MP_FH_cereb = MEDIPS.meth(MSet1=lib_2_MeDIP, CSet=CS,p.adj="BH",
diff.method="edgeR",
                        MeDIP=T, CNV=F, minRowSum=20)

save(MP_FC_cereb, file = "150WS_2gps_MP_FC_cereb")
save(MP_FH_cereb, file= "150WS_2gps_MP_FH_cereb")

# Male cerebellum C vs HBCDD
MP_MC_cereb = MEDIPS.meth(MSet1=lib_14_MeDIP, CSet=CS,p.adj="BH",
diff.method="edgeR",
                        MeDIP=T, CNV=F, minRowSum=20)
MP_MH_cereb = MEDIPS.meth(MSet1=lib_10_MeDIP, CSet=CS,p.adj="BH",
diff.method="edgeR",
                        MeDIP=T, CNV=F, minRowSum=20)

save(MP_MC_cereb, file = "150WS_2gps_MP_MC_cereb")
save(MP_MH_cereb, file= "150WS_2gps_MP_MH_cereb")

# Female brain stem C vs HBCDD
MP_FC_brstem = MEDIPS.meth(MSet1=lib_7_MeDIP, CSet=CS,p.adj="BH",
diff.method="edgeR",
                        MeDIP=T, CNV=F, minRowSum=20)
MP_FH_brstem = MEDIPS.meth(MSet1=lib_3_MeDIP, CSet=CS,p.adj="BH",
diff.method="edgeR",
                        MeDIP=T, CNV=F, minRowSum=20)

save(MP_FC_brstem, file = "150WS_2gps_MP_FC_brstem")
save(MP_FH_brstem, file= "150WS_2gps_MP_FH_brstem")

# Male brstem C vs HBCDD
MP_MC_brstem = MEDIPS.meth(MSet1=lib_15_MeDIP, CSet=CS,p.adj="BH",
diff.method="edgeR",
                        MeDIP=T, CNV=F, minRowSum=20)
MP_MH_brstem = MEDIPS.meth(MSet1=lib_11_MeDIP, CSet=CS,p.adj="BH",
diff.method="edgeR",
                        MeDIP=T, CNV=F, minRowSum=20)

save(MP_MC_brstem, file = "150WS_2gps_MP_MC_brstem")
save(MP_MH_brstem, file= "150WS_2gps_MP_MH_brstem")

#####
### Differential methylation Analysis
#####
dir.create("/mnt/pcpnfs/homedirs/dii6/6mA_HBCDD/CS-A/medips_MvF_files/DM")
setwd("/mnt/pcpnfs/homedirs/dii6/6mA_HBCDD/CS-A/medips_MvF_files/DM")

# female cerebellum C vs HBCDD

MP_F_CvH_cereb= MEDIPS.meth(MSet1=lib_6_MeDIP,MSet2=lib_2_MeDIP,
CSet=CS,p.adj="BH", diff.method="edgeR",
                        MeDIP=T, CNV=F,
                        minRowSum=20)
save(MP_F_CvH_cereb, file = "150WS_2gps_MP_F_CvH_cereb")
write.table(MP_F_CvH_cereb,"150WS_2gps_MP_F_CvH_cereb.txt",sep="\t")

MP_F_CvH_cereb.0.1s = MEDIPS.selectSig(results=MP_F_CvH_cereb, p.value=0.1,
adj=T,
                        ratio=NULL, bg.counts=NULL, CNV=F)

MP_F_CvH_cereb.0.05s = MEDIPS.selectSig(results=MP_F_CvH_cereb, p.value=0.05,
adj=T,
                        ratio=NULL, bg.counts=NULL, CNV=F)

head(MP_F_CvH_cereb.0.1s)

```



```

head(MP_F_CvH_cereb.0.05s)

save(MP_F_CvH_cereb.0.1s, file = "150WS_2gps_MP_F_CvH_cereb_0_1")
save(MP_F_CvH_cereb.0.05s, file = "150WS_2gps_MP_F_CvH_cereb_0_05")

write.table(MP_F_CvH_cereb.0.1s,"150WS_2gps_MP_F_CvH_cereb.0.1.txt",sep="\t")
write.table(MP_F_CvH_cereb.0.05s,"150WS_2gps_MP_F_CvH_cereb.0.05.txt",sep="\t")

# Male cerebellum C vs HBCDD

MP_M_CvH_cereb= MEDIPS.meth(MSet1=lib_14_MeDIP,MSet2=lib_10_MeDIP,
CSet=CS,p.adj="BH", diff.method="edgeR",
                        MeDIP=T, CNV=F,
                        minRowSum=20)
save(MP_M_CvH_cereb, file = "150WS_2gps_MP_M_CvH_cereb")
write.table(MP_M_CvH_cereb,"150WS_2gps_MP_M_CvH_cereb.txt",sep="\t")

MP_M_CvH_cereb.0.1s = MEDIPS.selectSig(results=MP_M_CvH_cereb, p.value=0.1,
adj=T,                                ratio=NULL, bg.counts=NULL, CNV=F)

MP_M_CvH_cereb.0.05s = MEDIPS.selectSig(results=MP_M_CvH_cereb, p.value=0.05,
adj=T,                                ratio=NULL, bg.counts=NULL, CNV=F)

head(MP_M_CvH_cereb.0.1s)
head(MP_M_CvH_cereb.0.05s)

save(MP_M_CvH_cereb.0.1s, file = "150WS_2gps_MP_M_CvH_cereb_0_1")
save(MP_M_CvH_cereb.0.05s, file = "150WS_2gps_MP_M_CvH_cereb_0_05")

write.table(MP_M_CvH_cereb.0.1s,"150WS_2gps_MP_M_CvH_cereb.0.1.txt",sep="\t")
write.table(MP_M_CvH_cereb.0.05s,"150WS_2gps_MP_M_CvH_cereb.0.05.txt",sep="\t")

# female brstem C vs HBCDD

MP_F_CvH_brstem= MEDIPS.meth(MSet1=lib_7_MeDIP,MSet2=lib_3_MeDIP,
CSet=CS,p.adj="BH", diff.method="edgeR",
                        MeDIP=T, CNV=F,
                        minRowSum=20)
save(MP_F_CvH_brstem, file = "150WS_2gps_MP_F_CvH_brstem")
write.table(MP_F_CvH_brstem,"150WS_2gps_MP_F_CvH_brstem.txt",sep="\t")

MP_F_CvH_brstem.0.1s = MEDIPS.selectSig(results=MP_F_CvH_brstem, p.value=0.1,
adj=T,                                ratio=NULL, bg.counts=NULL, CNV=F)

MP_F_CvH_brstem.0.05s = MEDIPS.selectSig(results=MP_F_CvH_brstem, p.value=0.05,
adj=T,                                ratio=NULL, bg.counts=NULL, CNV=F)

head(MP_F_CvH_brstem.0.1s)
head(MP_F_CvH_brstem.0.05s)

save(MP_F_CvH_brstem.0.1s, file = "150WS_2gps_MP_F_CvH_brstem_0_1")
save(MP_F_CvH_brstem.0.05s, file = "150WS_2gps_MP_F_CvH_brstem_0_05")

write.table(MP_F_CvH_brstem.0.1s,"150WS_2gps_MP_F_CvH_brstem.0.1.txt",sep="\t")
write.table(MP_F_CvH_brstem.0.05s,"150WS_2gps_MP_F_CvH_brstem.0.05.txt",sep="\t")

# Male brstem C vs HBCDD

MP_M_CvH_brstem= MEDIPS.meth(MSet1=lib_15_MeDIP,MSet2=lib_11_MeDIP,
CSet=CS,p.adj="BH", diff.method="edgeR",
                        MeDIP=T, CNV=F,
                        minRowSum=20)
save(MP_M_CvH_brstem, file = "150WS_2gps_MP_M_CvH_brstem")
write.table(MP_M_CvH_brstem,"150WS_2gps_MP_M_CvH_brstem.txt",sep="\t")

MP_M_CvH_brstem.0.1s = MEDIPS.selectSig(results=MP_M_CvH_brstem, p.value=0.1,
adj=T,                                ratio=NULL, bg.counts=NULL, CNV=F)

```

```

MP_M_CvH_brstem.0.05s = MEDIPS.selectSig(results=MP_M_CvH_brstem, p.value=0.05,
adj=T,
ratio=NULL, bg.counts=NULL, CNV=F)

head(MP_M_CvH_brstem.0.1s)
head(MP_M_CvH_brstem.0.05s)

save(MP_M_CvH_brstem.0.1s, file = "150WS_2gps_MP_M_CvH_brstem_0.1")
save(MP_M_CvH_brstem.0.05s, file = "150WS_2gps_MP_M_CvH_brstem_0.05")

write.table(MP_M_CvH_brstem.0.1s,"150WS_2gps_MP_M_CvH_brstem.0.1.txt",sep="\t")
write.table(MP_M_CvH_brstem.0.05s,"150WS_2gps_MP_M_CvH_brstem.0.05.txt",sep="\t")

#####
# Both sexes together
#####
setwd("/mnt/pcpnfs/homedirs/dii6/6mA_HBCDD/CS-A/medips_sets")

Cereb_2S_H = c(lib_2_MeDIP, lib_10_MeDIP)
Cereb_2S_C = c(lib_6_MeDIP, lib_14_MeDIP)

Brstem_2S_H = c(lib_3_MeDIP, lib_11_MeDIP)
Brstem_2S_C = c(lib_7_MeDIP, lib_15_MeDIP)

#           Methylation profiles
#
dir.create("/mnt/pcpnfs/homedirs/dii6/6mA_HBCDD/medips_2S_files")
setwd("/mnt/pcpnfs/homedirs/dii6/6mA_HBCDD/medips_2S_files")

#
#           Differential methylation
#
#           2 sex cerebellum C vs HBCDD

MP_2S_CvH_cereb= MEDIPS.meth(MSet1=Cereb_2S_C,MSet2=Cereb_2S_H,
CSet=CS,p.adj="BH", diff.method="edgeR",
MeDIP=T, CNV=F,
minRowSum=20)
save(MP_2S_CvH_cereb, file = "150WS_2gps_MP_2S_CvH_cereb")
write.table(MP_2S_CvH_cereb,"150WS_2gps_MP_2S_CvH_cereb.txt",sep="\t")

MP_2S_CvH_cereb.0.1s = MEDIPS.selectSig(results=MP_2S_CvH_cereb, p.value=0.1,
adj=T,
ratio=NULL, bg.counts=NULL, CNV=F)

MP_2S_CvH_cereb.0.05s = MEDIPS.selectSig(results=MP_2S_CvH_cereb, p.value=0.05,
adj=T,
ratio=NULL, bg.counts=NULL, CNV=F)

head(MP_2S_CvH_cereb.0.1s)
head(MP_2S_CvH_cereb.0.05s)

save(MP_2S_CvH_cereb.0.1s, file = "150WS_2gps_MP_2S_CvH_cereb_0.1")
save(MP_2S_CvH_cereb.0.05s, file = "150WS_2gps_MP_2S_CvH_cereb_0.05")

write.table(MP_2S_CvH_cereb.0.1s,"150WS_2gps_MP_2S_CvH_cereb.0.1.txt",sep="\t")
write.table(MP_2S_CvH_cereb.0.05s,"150WS_2gps_MP_2S_CvH_cereb.0.05.txt",sep="\t")

#           2 sex brstem C vs HBCDD

MP_2S_CvH_brstem= MEDIPS.meth(MSet1=Brstem_2S_C,MSet2=Brstem_2S_H,
CSet=CS,p.adj="BH", diff.method="edgeR",
MeDIP=T, CNV=F,
minRowSum=20)
save(MP_2S_CvH_brstem, file = "150WS_2gps_MP_2S_CvH_brstem")
write.table(MP_2S_CvH_brstem,"150WS_2gps_MP_2S_CvH_brstem.txt",sep="\t")

MP_2S_CvH_brstem.0.1s = MEDIPS.selectSig(results=MP_2S_CvH_brstem, p.value=0.1,
adj=T,
ratio=NULL, bg.counts=NULL, CNV=F)

```

```

      MP_2S_CvH_brstem.0.05s      =      MEDIPS::selectSig(results=MP_2S_CvH_brstem,
p.value=0.05, adj=T,
                                ratio=NULL, bg.counts=NULL, CNV=F)

      head(MP_2S_CvH_brstem.0.1s)
      head(MP_2S_CvH_brstem.0.05s)

      save(MP_2S_CvH_brstem.0.1s, file = "150WS_2gps_MP_2S_CvH_brstem_0.1")
      save(MP_2S_CvH_brstem.0.05s, file = "150WS_2gps_MP_2S_CvH_brstem_0.05")

write.table(MP_2S_CvH_brstem.0.1s,"150WS_2gps_MP_2S_CvH_brstem.0.1.txt",sep="\t")
write.table(MP_2S_CvH_brstem.0.05s,"150WS_2gps_MP_2S_CvH_brstem.0.05.txt",sep="\t")

```

8. Zusammenfassung

Hexabromocyclododecan (HBCDD) ist ein bromiertes Flammschutzmittel, das in vielen hergestellten Materialien verwendet wird und aus einer technischen Mischung von 3 Hauptisomeren α , β und γ besteht, wobei das α Isomer hauptsächlich in Lebensmitteln und in biologischen Abteilungen vorkommt. Da HBCDD in der Umwelt, Lebensmitteln und menschlichem Gewebe vorkommt, sind Folgen für die menschliche Gesundheit zu erwarten, insbesondere wenn die Exposition während der frühen Entwicklungsphase stattfindet.

Ausgehend von einer früheren Studie über die kurzfristigen Auswirkungen der perinatalen Exposition gegenüber dem Umweltschadstoff HBCDD [1] untersuchte das aktuelle Projekt die entsprechenden Gehirnstrukturen aus den bisherigen Ergebnissen, welche Beeinträchtigungen des Bewegungsapparates sowie endokrine Störungen hervorbrachten. Ziel dieses Projektes war es, die langfristigen Auswirkungen der Schadstoffbelastung und der Auswirkungen auf die Neuroinflammation sowie auf das epigenetische Profil zu identifizieren. Weibliche Wistar-Ratten wurden während der Schwangerschaft und Stillzeit mit α -HBCDD kontaminierten Eiern gefüttert. Daher wurden die Nachkommen über einen Zeitraum von 42 Tagen dem Schadstoff ausgesetzt. Da die Menge an HBCDD nach der Exposition des Menschen berechnet wurde, was zu einer Verabreichung von 66 ng/kg/Tag und 42 Tagen bei Laborratten etwa 3 Jahren beim Menschen gleichgesetzt sind [2], gilt dies als früher Stressfaktor. Da das frühe Leben eine sehr kritische Phase ist und den Gesundheitsverlauf im späteren Leben beeinflussen kann [3], müssen die Auswirkungen der Schadstoffbelastung genauer untersucht werden.

Die vorliegende Studie konzentrierte sich auf die entnommenen Gehirne von PND1, PND14 und PND270. So wurden die Folgen einer frühzeitigen Schadstoffbelastung zu drei verschiedenen Zeitpunkten, von der Geburt bis zum Erwachsenenalter, untersucht. Nachdem an PND1-Hirnen gezeigt wurde, dass HBCDD die Plazenta und die Hirn-Blut-Schranke passieren kann, wurden die Neuroinflammationsstufen bewertet. Es wurden signifikant erhöhte Neuroinflammationswerte im Kortex beobachtet, was die Hypothese fördert, dass die Schadstoffbelastung die Gehirnentwicklung und -funktion von Anfang an beeinflussen kann.

Auf der epigenetischen Ebene dieses Projekts wurde 6-Methyladenosin als echte epigenetische Marke identifiziert. Zuerst wurde die Existenz durch LC-MS/MS bestätigt, dann wurden dynamische Veränderungen als Reaktion auf die α -HBCDD-Exposition durch DotBlots analysiert. Eine deutliche Tendenz zu einem Rückgang der 6mA Abundanz in α -HBCDD-Gruppen im Vergleich zu Kontrollgruppen wurde beobachtet. Ein visueller Nachweis des Auftretens von 6mA im neuronalen Gewebe von PND270 wurde zum ersten Mal durch immunohistochemische Färbungen gewonnen. Schließlich wurden PND14-Proben immunopräzipitiert und die Illumina®-Sequenzierung durchgeführt. Dies führte zu einer Auflistung der differentiell methylierten Regionen (DMR) auf jedem Chromosom. Es wurden erhebliche Unterschiede in der Anzahl der DMRs erhoben, was zeigt, dass die α -HBCDD-Exposition Unterschiede in den Methylierungsprofilen auslöst. Im Anschluss daran sollten entsprechende Gene untersucht und die Auswirkungen auf die Genexpression definiert werden. Insgesamt kann α -HBCDD also nicht nur in das sich entwickelnde Gehirn eindringen und es beeinflussen, sondern beeinflusst auch deutlich epigenetische Modifikationen.

Schlüsselwörter: Frühes Leben, persistente organische Schadstoffe, HBCDD, Epigenetik, Neuroinflammation, 6-Methyladenosin

9. Eidesstattliche Erklärung

Ich erkläre hiermit an Eides Statt, dass ich die vorliegende Arbeit selbständig und ohne Benutzung anderer als der angegebenen Hilfsmittel und Quellen angefertigt habe. Die aus fremden Quellen direkt oder indirekt übernommenen Gedanken sind als solche kenntlich gemacht. Die Arbeit wurde bisher in gleicher oder ähnlicher Form keiner anderen Prüfungsbehörde vorgelegt und auch noch nicht veröffentlicht.

Ich erkläre mich mit der Archivierung der vorliegenden Masterarbeit einverstanden.

Datum

Unterschrift

Wien den 5.06.2019

Sarah Roth